InGaN–GaN Multiple Quantum Wells for Green LEDs on Si

Benjamin A. Reeves, Ze Zhang
Mentors: Dr. Michael Grundmann (X), Dr. Dong Lee (QMAT),
Dr. Xiaoqing Xu (SNF)

1 Introduction

III-N semiconductors offer direct electronic room temperature bandgaps from 0.7 eV to 6.3 eV, as well as a host of other excellent electronic properties. Vurgaftman and Meyer [1] and Vurgaftman et al. [2] provide excellent reviews of III-V band parameters, with the former including important refinements to the bandgap of InN. The III-Ns are extraordinary for other reasons as well. They have high electron saturation velocities, high breakdown voltages, internal spontaneous and piezoelectric polarizations on the order of $1\,\mathrm{V\,nm^{-1}}$, and high thermal conductivity.[3,4] Like many nitrides, they are hard, strong, brittle materials with melting temperatures far above their decomposition temperatures; equilibrium N_2 vapor pressures can reach $\sim 10^4$ atm and the materials tend to separate into metal and nitrogen at elevated temperatures.[5] This, among other reasons, is why synthesis of bulk, III-N, single-crystal substrates is difficult; the highest quality III-N substrates are generally not commercially available, and relatively low-quality GaN wafers typically cost $\sim$ \$1000 per 5 cm diameter wafer.

The high cost or unavailability of bulk, single-crystal III-N substrates has led to heavy development of III-N heteroepitaxy, i.e., the growth of III-N single crystal thin films on substrates whose thermal, structural, and chemical properties are different from the III-Ns. In particular, the abundance of single-crystal Si wafers, coupled with a push towards integrating III-V materials into Si-based optoelectronic devices, led to significant work on III-N/Si heteroepitaxy. Homoepitaxy and growth on other substrates is important but not addressed here. Furthermore, we focus on organometallic chemical vapor deposition (MOCVD) of Ga-face (wurtzite) GaN because it is the growth technique used in this work. Reviews of GaN and other III-N semiconductor properties and semiconductor devices may be found in Willardson and Weber [3] and Moustakas and Paiella [6].

$In_xGa_{1-x}N$–GaN multiple quantum wells can be constructed such that they emit green photons directly and are being studied for high-efficiency green LEDs. Green LEDs suffer from efficiency issues not found in other visible-range LEDs, however, an issue often referred to as the "green gap".[6,7] Device specifics vary—and, while possible, determining precise In values in InGaN quantum wells is neither straightforward[8] nor pursued further here—but it is reasonable to say that green $In_xGa_{1-x}N$ requires $x \approx 0.2$–0.3, and that such high In concentrations are difficult to achieve in practice without introducing significant material issues. These material issues include InGaN decomposition, alloy fluctuations, spatial gradients in the electrical potentials and strain states (giving rise to additional electric fields via piezoelectricity), dislocations, and point defects.[9–11] Further, InGaN–GaN thin films will vary in quality within a single multiple quantum well (MQW) sequence,[12] and localization effects can produce counterintuitive results about the material performance.[11]

There are clearly many opportunities to study, understand, and improve high-In content InGaN

thin films, and incorporating these films into devices on Si substrates is also worthwhile. We therefore decided to establish baseline organometallic chemical vapor deposition (MOCVD) recipes for green LED MQW structures on Si. We manipulated process variables to establish a range of growth conditions to produce LED structures with luminescence near 530 nm. Further, we demonstrated promising avenues towards improving the optical properties of these structures. These results provide a baseline for future MOCVD users wishing to fabricate high-In InGaN thin films and green MQW structures on Si substrates.

Experimental techniques are described in Section 2. The main results are presented and discussed in Section 3 and we conclude in Section 4. The sequential description of our experiments and choices for the class are given in Section A, with all additional experimental data and computer code in the appendices.

2 Experimental Methods

MOCVD was performed using an Aixtron CCS (close-coupled showerhead) computer-controlled MOCVD system. The precursors were carried in purified H_2 and N_2 process gases. Purified NH_3 and 100 ppm SiH_4 in H_2 were used as hydride precursors. Trimethyl indium (TMIn), trimethyl gallium (TMGa), triethyl gallium (TEGa), trimethyl aluminum (TMAl), and bis-cyclopentadienyl magnesium (Cp_2Mg) were used as organometallic (MO) precursors. Water baths for the MO precursors were set to 18 °C, 2 °C, 10 °C, 20 °C, and 25 °C, and precursor pressures set to 1200 mbar, 1900 mbar, 1200 mbar, 1300 mbar, and 1200 mbar, respectively. A 100 mm±0.1 mm diameter, 750 µm±25 mm thick, $< 111 > \pm 0.1^\circ$, p-type, $<1\,\Omega\,$cm Si wafer was used as a substrate to grow the LED MQW structure up to the n-GaN layer. This buffer wafer was then kept in the MOCVD glovebox and cleaved with a diamond scribe as required to produce ∼1 cm growth pieces for the other growths. All molar flow rates were calculated using vendor-provided empirical relations between vapor pressures and bubbler conditions as well as process gas flow rates.

Full recipe details are available upon request. All temperatures in this report are setpoint temperatures, but emissivity-corrected laser pyrometer measurements for true surface temperatures during growth are also available. Briefly, the Si was baked in H_2, followed by a bake in SiH_4. Then, a low-temperature AlN nucleation layer (LT-AlN) was grown on the Si, followed by high-temperature AlN (HT-AlN), $Al_{0.8}Ga_{0.2}N$, $Al_{0.5}Ga_{0.5}N$, $Al_{0.2}Ga_{0.8}N$, and n-GaN. This formed the buffer from which pieces were cleaved. For pieces, each specimen was first baked to remove surface contamination. Then, a nominally undoped GaN quantum barrier was grown, followed by 5 nominally (3 nm, 9 nm) $In_xGa_{1-x}N$–GaN quantum well/quantum barrier pairs. A ∼1 nm GaN cap was grown on each InGaN layer prior to the GaN barrier. This cap was grown at the InGaN growth temperature in cases where temperature changed during the quantum well/quantum barrier growths. Finally, a 1.0×10^2 nm p-GaN layer was grown at 1040 °C, followed by a ∼1 nm p^+-GaN capping layer.

The main photoluminescence experiments presented here were performed using a Horiba FluoroLog Fluorometer. Light from a 450 W Xe arc lamp and a double-Blazed-grating monochromator produced 375 nm light. This light was incident the thin film specimens at nominally 60° from the surface normals, and also on a silicon photodetector. Luminescence was dispersed with a second double-Blazed-grating monochromator, and another Si photodetector measured intensity as a function of wavelength. The measured intensity was normalized by the signal of the incident light Si detector, and an instrument-specific correction algorithm was used to remove known artifacts. The data presented in Section 3 were measured as a complete set using constant fluorometer slit widths

and nominally constant measurement angle and illuminated area. Additional photoluminescence in Section A was measured on two different free space laser setups using a 375 nm laser excitation source; details are available upon request but the systems have since been deconstructed. Ultraviolet illuminated images were taken with a digital camera while illuminating the specimens with a conventional 365 nm UV light source (i.e. a "black light"). Finally, in two cases, a diamond scribe was used to scratch into the films, and then a ∼0.1 mm to 1 mm diameter In contact was melted on the scratched surface. Another In contact was melted on the p^+-GaN. A ∼10 V direct current source was connected to the contacts and the resulting light was imaged with a digital camera. In some cases, the n-GaN contact fell off, and contact was made directly between the probe and the film.

Scanning electron microscopy (SEM) was performed with a FEI Magellan using specimens cleaved from growth pieces. Specimens were plasma cleaned during the measurement but no additional cleaning procedures were used prior to imaging. Transmission electron microscopy (TEM) specimens were prepared with focused ion beam (FIB) milling on a FEI Helios NanoLab 600i Dual Beam FIB/SEM. First, E-beam C and I-beam Pt were deposited as a protective layer. Then, using a 30 kV accelerating voltage and up to 40 µA ion currents, the cross-section specimen was defined using two parallel trenches milled such that they intersected in the Si. Then, the section was lifted out using an OmniProbe micromanipulator. The specimens was welded with Pt onto a TEM grid. Finally, the sample was thinned using a 10 kV ion beam accelerating voltage until the specimen was electron-transparent. TEM was performed using a FEI Tecnai with a 200 kV accelerating voltage. All images are either bright field transmission electron micrographs or bright/dark field scanning transmission electron micrographs.

X-ray diffraction was performed on an X'Pert PRO X-ray diffractometer using a Cu K-α source and hybrid monochromator. Specimens were taped to glass and the instrument position was calibrated using known Bragg peak prior to measurements. For the main work, we used either a triple-axis point detector for rocking and symmetric-radial scans (on the (002) GaN peak unless otherwise noted), and a PIXIS line detector for reciprocal space maps (on the $(\bar{1}05)$ peak unless otherwise noted). Finally, atomic force microscopy (AFM) was performed with a Park NX-10 operated in non-contact ("tapping") mode using an ACTA probe.

3 Main Results and Discussion

We performed a total of 17 successful MOCVD growths during the course. The growths, some details, and the names by which we refer to the respective specimens are listed in Table 3. The nominal structure of all specimens discussed here is shown in Figure 1. This system is designed such that, under forward bias, carriers in the doped GaN layers move into the quantum wells, becoming localized and recombine to produce light. Typically, a high-bandgap electron blocking layer would be grown near the upper quantum well (QW) interface, but that was not pursued here. In general, the buffer structure we adopted (from a nominally i-GaN buffer recipe with no modification for n-GaN) resulted in some cracks in the thin films. These cracks tended to occur near the edges of the film and we often did not see any cracks while performing scanning electron microscopy over cm-scale pieces. That being said, cracks were not studied in more detail during these experiments, and wafer scale device production would require a separate buffer optimization study. An electron micrograph of the buffer surface (taken on a different electron microscope (FEI Sirion) than the rest of the electron micrographs (FEI Magellan)) is shown in Figure 2.

Typical measurements for our stacks are shown in the scanning electron micrograph in Figure 6.

Transmission electron micrographs in Figures 3 and 4 show this nominal device structure and the MQWS. The MQWs for this specimen appeared to have gross well-width fluctuations.[11], though this isn't as pronounced in other images such as Figure 5; a more thorough and concentrated TEM study would be required to better characterize the MQWs in our specimens. The specimen in Figures 5 and 4 was the thin QW specimen, a specimen for which we used 2/3 the normal QW growth time in order to try to make the thin films coherently strained to the n-GaN. Because it has 2.5 nm thick QWs, we estimate that all other growths have a QW thickness between 3.5 nm to 4 nm. Further, X-ray reciprocal space mapping for the thin QW specimen, shown in Figure 7, shows that the thin films were not coherently strained to GaN. (0002) superlattice fringes showed identical alignment to the GaN peak within the resolution of these measurements, however, and so we conclude that the in-plane atomic spacing for the InGaN is different than the n-GaN. Assuming a linear change in lattice constant with In-incorporation, the thin film appears partially strained, but it is likely a combination of the effects in high-In InGaN as discussed in Section 1. Because of the linear relationship between strain energy and layer thickness for a coherently strained film, and because this thin QW growth used 2/3 the InGaN growth time of the other films, it is unlikely that any QWs here are coherently strained. Many specimens with the normal QW growth time were measured with reciprocal space mapping and none of them were coherently strained, as shown in the appendix.

Referring to Table 3, all X °C Y% specimens form a two-factor experiment for nominally operating MQW LED thin film structures. The two factors are the molar flow ratios of the TMIn and total group III precursors during the InGaN growth and the InGaN growth temperature T. The photoluminescence results for these specimens are shown in Figure 8. These experiments used low-temperature (1040 °C) p-GaN and shorter p-GaN growth times to prevent decomposing the InGaN during the p-GaN growth. The 820 °C 75% specimen used a 120 nm thick p-GaN cap grown at 1035 °C because it was the second-to-last growth in a series of specimens used to produce 100 nm of 1040 °C p-GaN. The temperature and growth time is close enough to the other 1040 °C, 100 nm growths, however, that the specimen is comparable to the others. The experiment shows that the peak photoluminescence signals are near to and bracket 530 nm. Increasing the TMIn flow rate increased the amount of In in the specimens, i.e. red-shifted them, demonstrating that the In incorporation rate is not saturated at these growth conditions. Increasing T resulted in less In incorporation and red-shifted the specimens as expected. We note that the peak wavelengths and full-width, half-maximum values shown in Figure 8 came from photoluminescence data with characteristic etalon-like minima and maxima due to reflection at the interfaces and optical length scale, single-crystal thin films, as seen in Figure 9. No attempt was made to fit the data or correct for these fringes; the peak wavelength was found and then we determined the largest wavelength range between points with approximately half of this value.

The real specimens fluorescing under UV light are shown in Figure 10. The edges of the specimens appeared yellow, presumably due to the lower temperature near the edges leading to more In incorporation. There were no observed color gradients across the specimens, outside of the growth around e.g. contaminant particles, but photoluminescence mapping would At least two of the structures emitted visible light when an electric potential was applied across the n- and p-GaN layers, as shown in Figures 11 and 12.

The two-factor experiments were performed with a constant T for the quantum barriers (QBs) and QWs. This is not typical, however, and increasing T for the GaN QBs can change the interface and electronic quality of the GaN for better LED performance. We adopted a blue LED recipe to grow our stacks, and this recipe used a higher QB growth temperature; i.e., the temperature was

changed and stabilized at each QB-QW interface. In order to keep the results consistent, to anticipate future growths where a hold time was required for higher T QB growth, and not understanding that hold times at interfaces can be detrimental to device performance due to the accumulation of contaminants, we kept the hold times in for growths with constant QB/QW T. Figure 9 shows the result of two additional experiments performed with the 810 °C 75% recipe. For one, the hold time was reduced by approximately an order of magnitude at the interfaces. This growth produced a specimen with higher photoluminescence efficiency, consistent with the idea of contaminants at the interfaces. The peak wavelength was red-shifted, consistent with reduced InGaN decomposition, higher In incorporation, and perhaps fluctuation in In incorporation between growths for a given recipe. Either way, when the hold periods were restored to allow for T stabilization during higher-temperature QB growths, the improvement in peak photoluminescence efficiency persisted. The specimen blue shifted slightly, consistent with InGaN decomposition at higher temperatures. It is reasonable to use the results shown in Figure 8 to choose growth conditions for which a single-factor, QB temperature study could produce the highest green photoluminescence signal. It is also reasonable to expect that the specimens grown here could be etched and contacted to produce working green LEDs for efficiency characterization and future optimization.

4 Conclusion

We developed growth recipes and demonstrated green InGaN–GaN MQW LED thin film structures on Si substrates. A two-factor experiment was conducted that produced LED structures with wavelengths from approximately 490 nm to 550 nm and from which future green LED device processes may be designed. The films were determined to be incoherent with respect to n-GaN. Increasing the quantum barrier temperature blue-shifted the photoluminescence and increased photoluminescence by about a factor of 10. Devices appeared green in electroluminescence and under UV illumination.

Table 1: Summary of growths as of May 27$^{\text{th}}$, 2018. Molar flow rates and "Name" temperatures are for the InGaN quantum wells, if applicable, with unit µmol min^{-1}. All p-GaN caps capped with p$^+$-GaN. All temperatures are setpoints.

Name	Process ID	$\dot{m}_{\text{TMIn}}$	$\dot{m}_{\text{TEGa}}$	Cap	Notes
Buffer	572	-	-	-	Si-buffers + n-GaN, cleaved and used for 574-599
First 820 °C MQW	574	7.1	2.3	100 nm n-GaN	T irreproducible due to manual adjustment for target true T
800 °C MQW	578	7.1	2.3	50 nm n-GaN	
820 °C MQW	580	7.1	2.3	-	
820 °C Purple LED	582	7.1	2.3	250 nm, 1125 °C p-GaN	
820 °C 75%	586	7.1	2.3	130 nm, 1035 °C p-GaN	T irreproducible due to manual adjustment for target true T
800 °C 75%	590	7.1	2.3	100 nm, 1040 °C p-GaN	
810 °C 75%	595	7.1	2.3	100 nm, 1040 °C p-GaN	Chamber vented to atmosphere and regenerated before run.
810 °C 90%	597	20.8	2.3	100 nm, 1040 °C p-GaN	
810 °C 70%	599	5.4	2.3	100 nm, 1040 °C p-GaN	
Buffer	600	-	-	-	Si-buffers + n-GaN, cleaved and used for
800 °C 70%	612	5.4	2.3	100 nm, 1040 °C p-GaN	
Failed thin QW	616	7.1	2.3	100 nm, 1040 °C p-GaN	Used 2/3 growth time for QWs. Color gradient under UV lamp suggested particle under specimen.
Thin QW	620	7.1	2.3	100 nm, 1040 °C p-GaN	Repeated 612, no gradient.
820 °C 80%	622	9.2	2.3	100 nm, 1040 °C p-GaN	
Short hold time	626	7.1	2.3	100 nm, 1040 °C p-GaN	Reduced hold time at InGaN–GaN interfaces
High temperature barrier	630	7.1	2.3	100 nm, 1040 °C p-GaN	$\Delta T = 50$ °C for quantum barriers

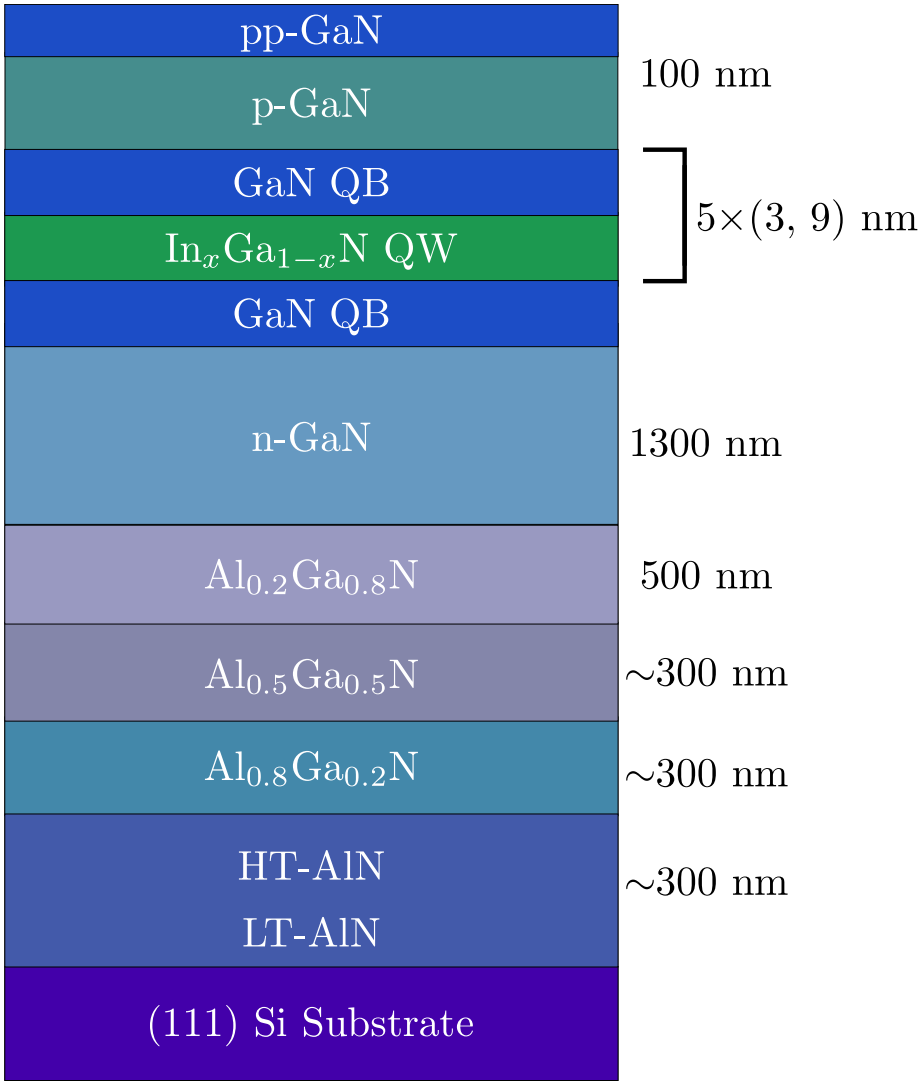

Figure 1: A schematic of the LED MQW structure discussed for the two-factor experiment. We made contact with two of the six structures and both turned on and produced visible green light.

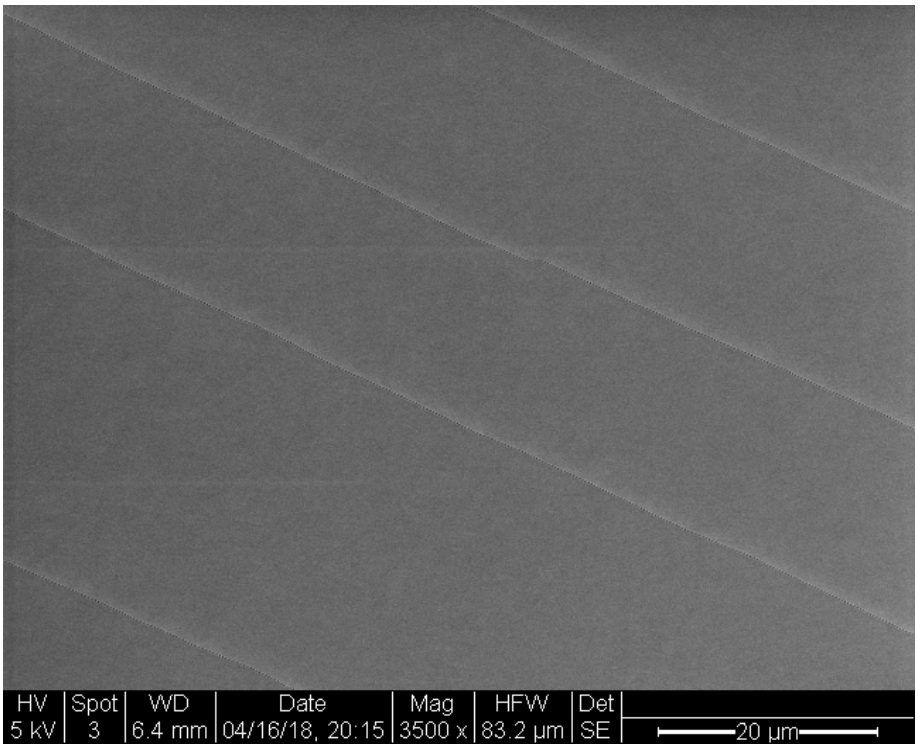

Figure 2: A plan view of a buffer surface showing cracks. We did not typically encounter cracks in SEM. This suggests that the buffer structure may not need significant modification for wafer scale GaN-on-Si thin films.

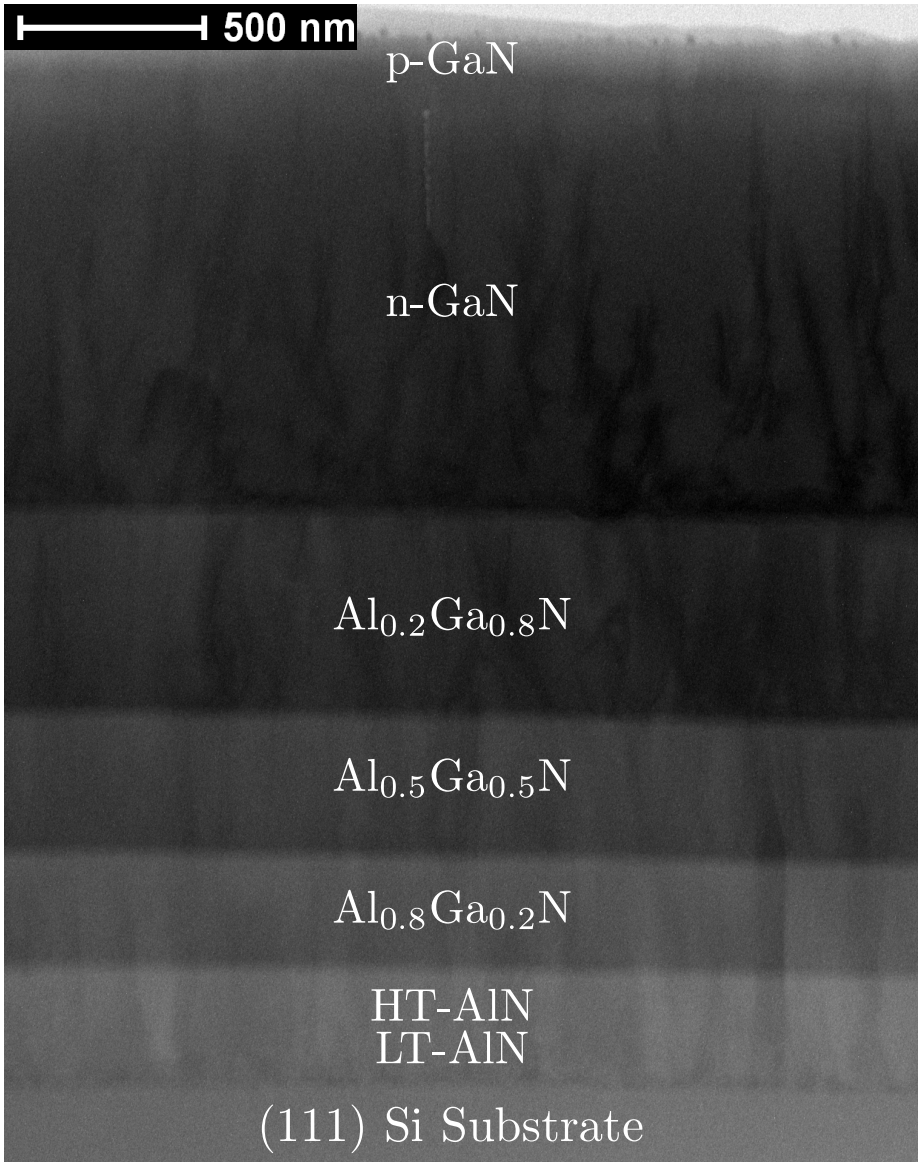

Figure 3: A transmission electron micrograph showing the cross section of an LEW MQW stack on Si.

Figure 4: The MQWs show gross well width fluctuations, though a more careful TEM study would be necessary to improve confidence.

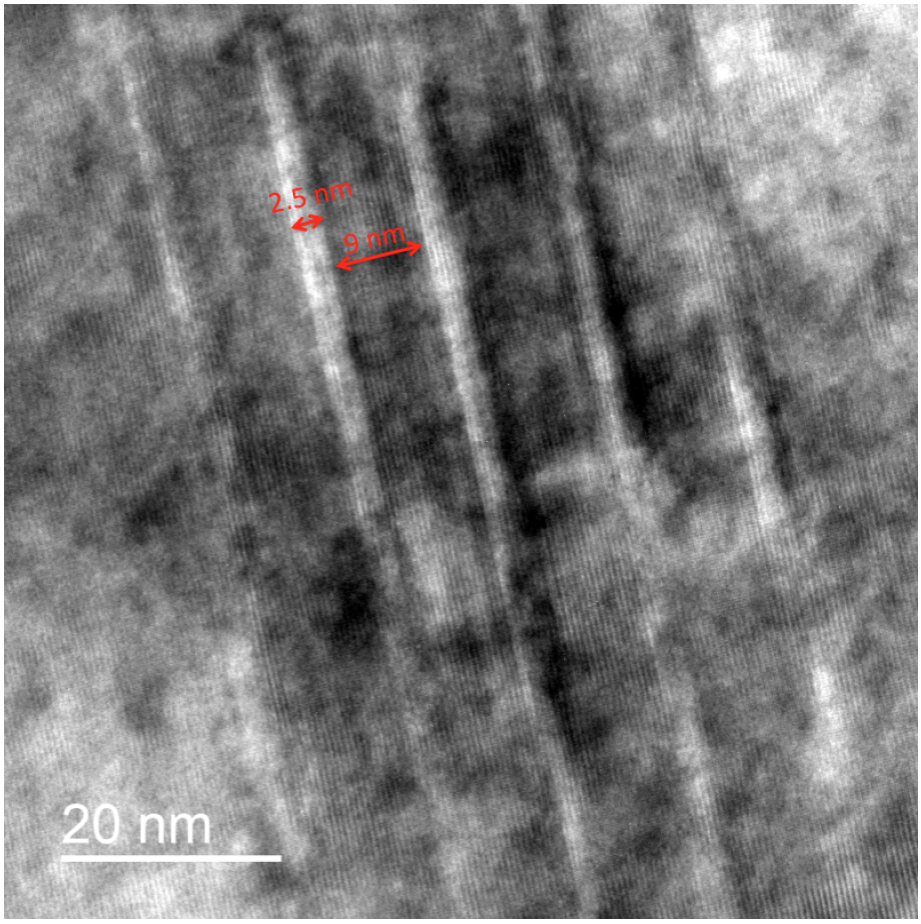

Figure 5: Transmission electron micrograph showing a clearer picture and measurements of the MQWs. Because this specimen used 2/3 the growth time for its QWs, we estimate that the other specimens had 3.5 nm to 4 nm QW thicknesses.

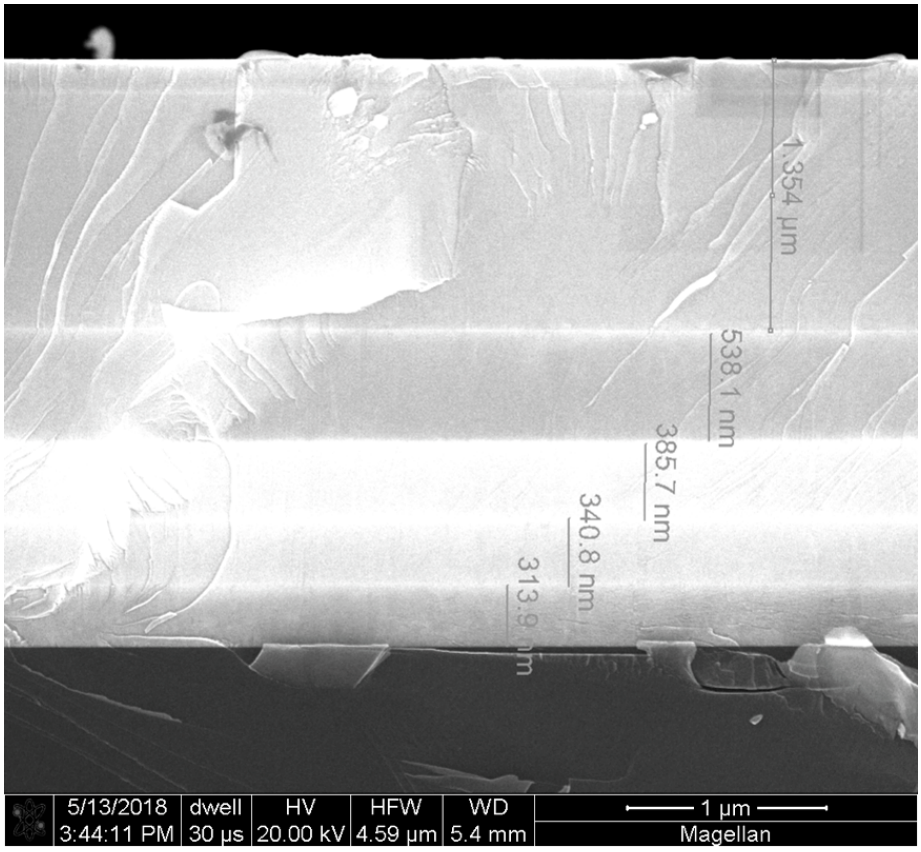

Figure 6: Scanning electron micrograph of a typical stack.

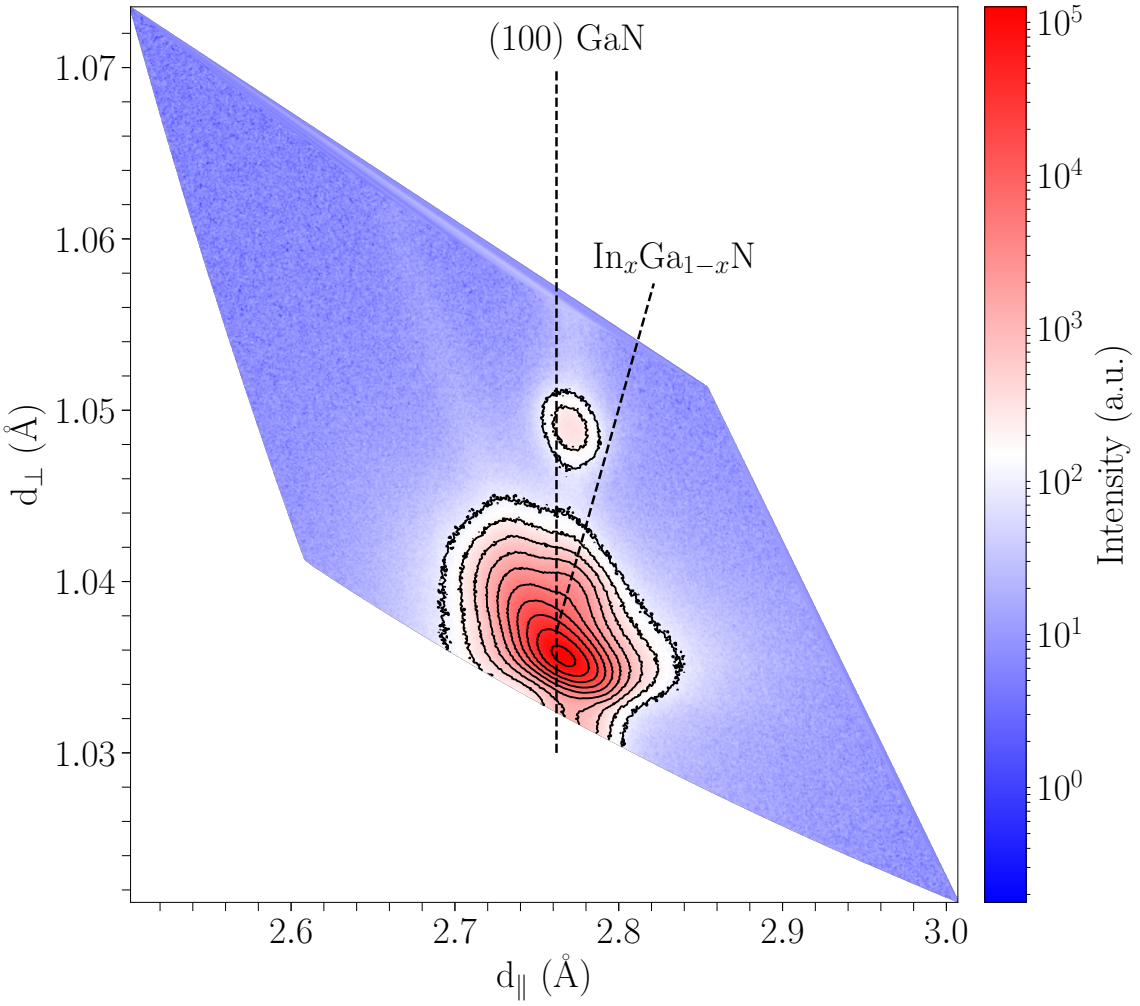

Figure 7: ($\bar{1}05$) X-ray reciprocal space map of the thin QW specimen, which used InGaN with nomincally 2/3 thickness of other specimens. Not all specimens were measured in X-ray diffraction, but it is likely that none of them were coherently strained if the thinnest one is not.

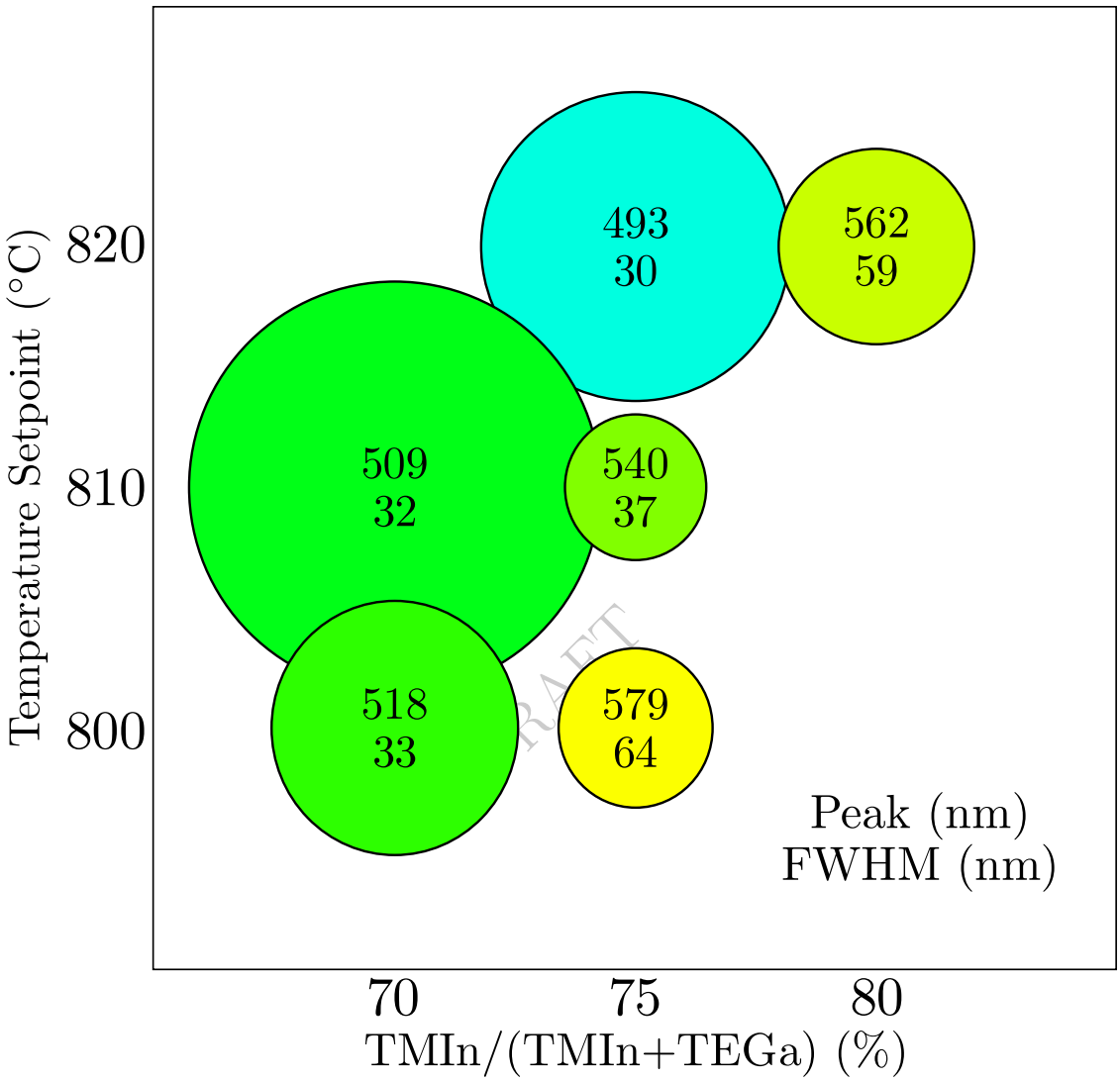

Figure 8: Photoluminescence results of the two-factor experiment. Colors represent the peak wavelength color, and the associated wavelength and full-width half maximum of the peak are listed in the circles. The ordering of the peak intensity is represented by the relative size of the circles, though the ratio of the largest and smallest intensity ($\sim 10^2$) is not reflected in the area of the circles.

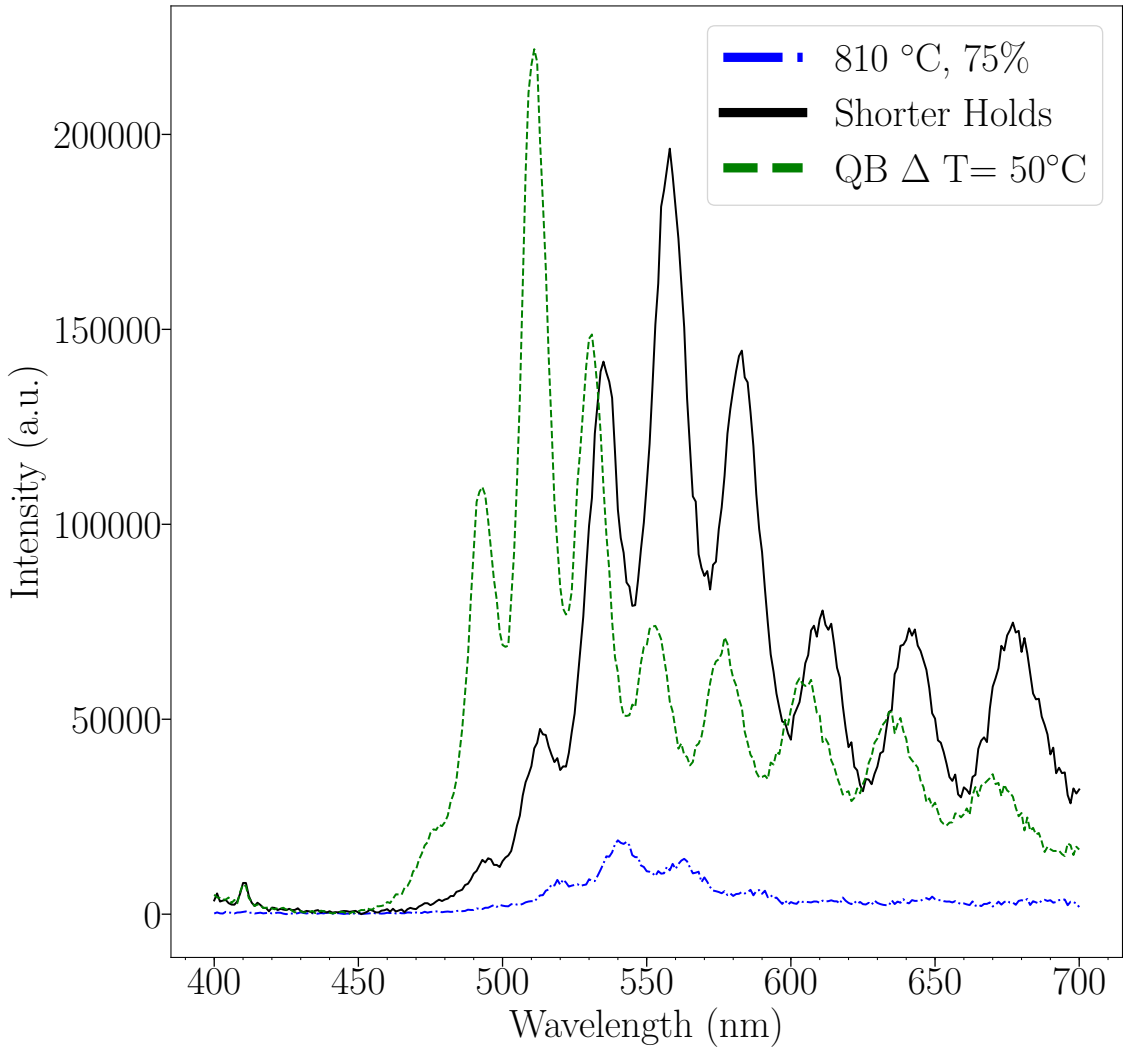

Figure 9: The 810 °C 75% specimen photoluminescence, along with the same InGaN growth conditions made with reduced hold time at the interface, and with a higher QB temperature. The shifts relative to the two-factor experiments can help future users predict conditions for high-efficiency green emission.

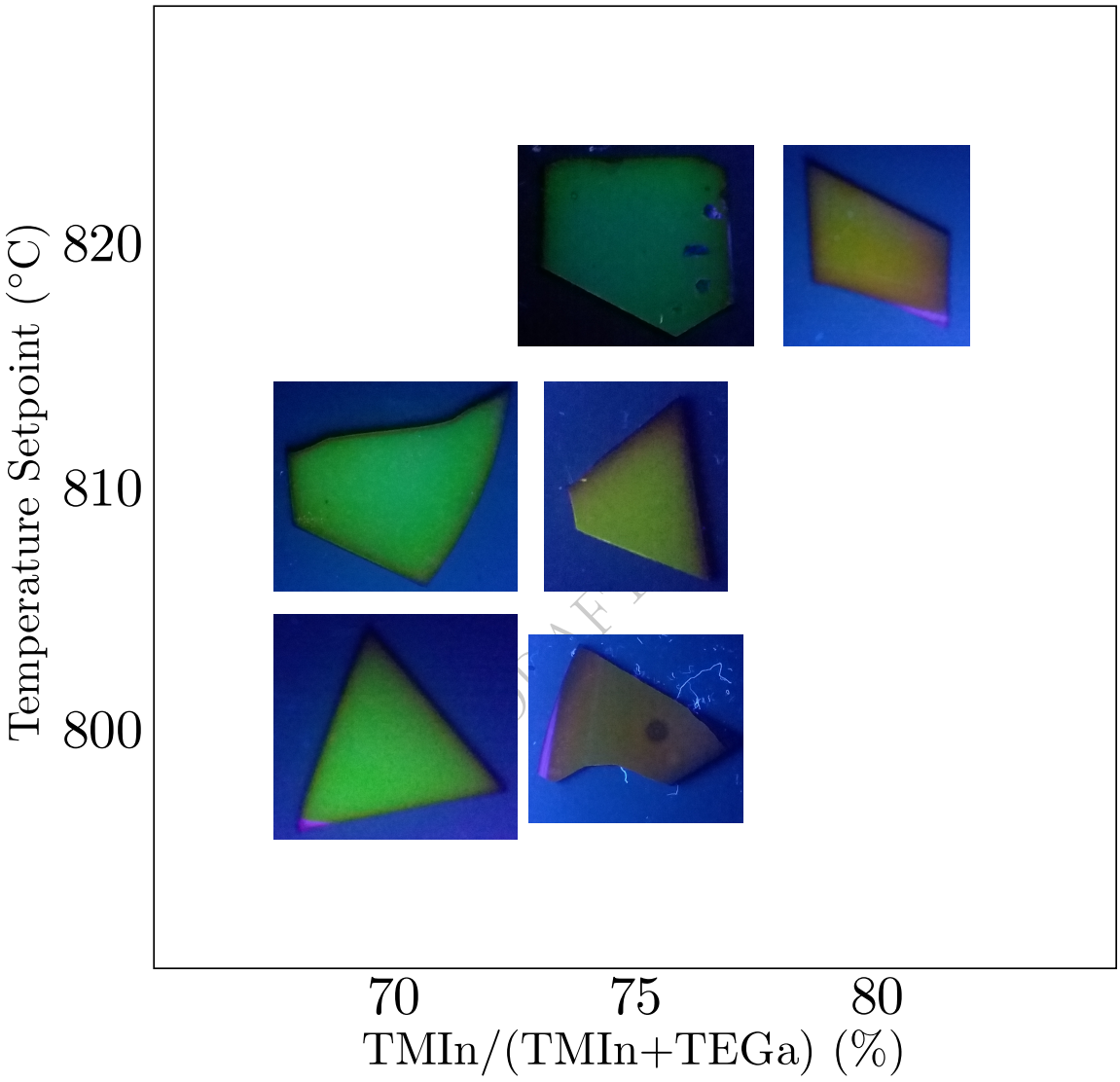

Figure 10: The two-factor specimens under 365 nm illumination. In contacts are seen on the 820 °C 75% specimen.

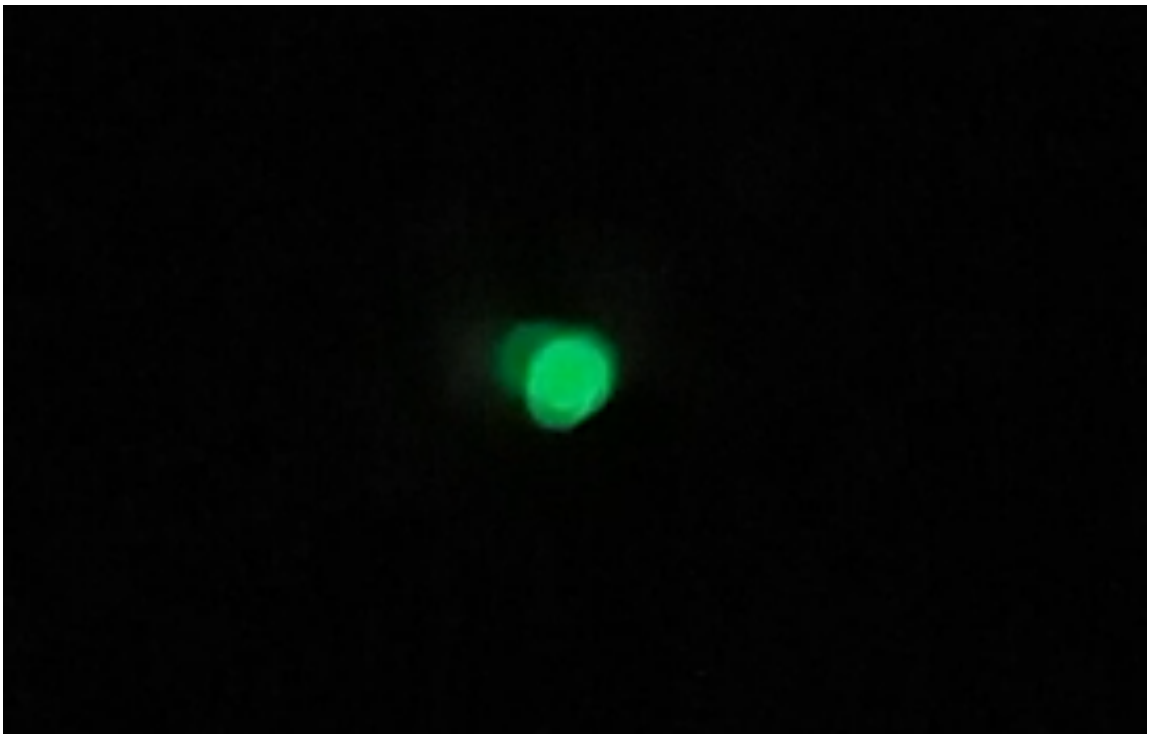

Figure 11: Electroluminescence from the 810 °C 70% specimen. The autofocus would not adjust in the dark room.

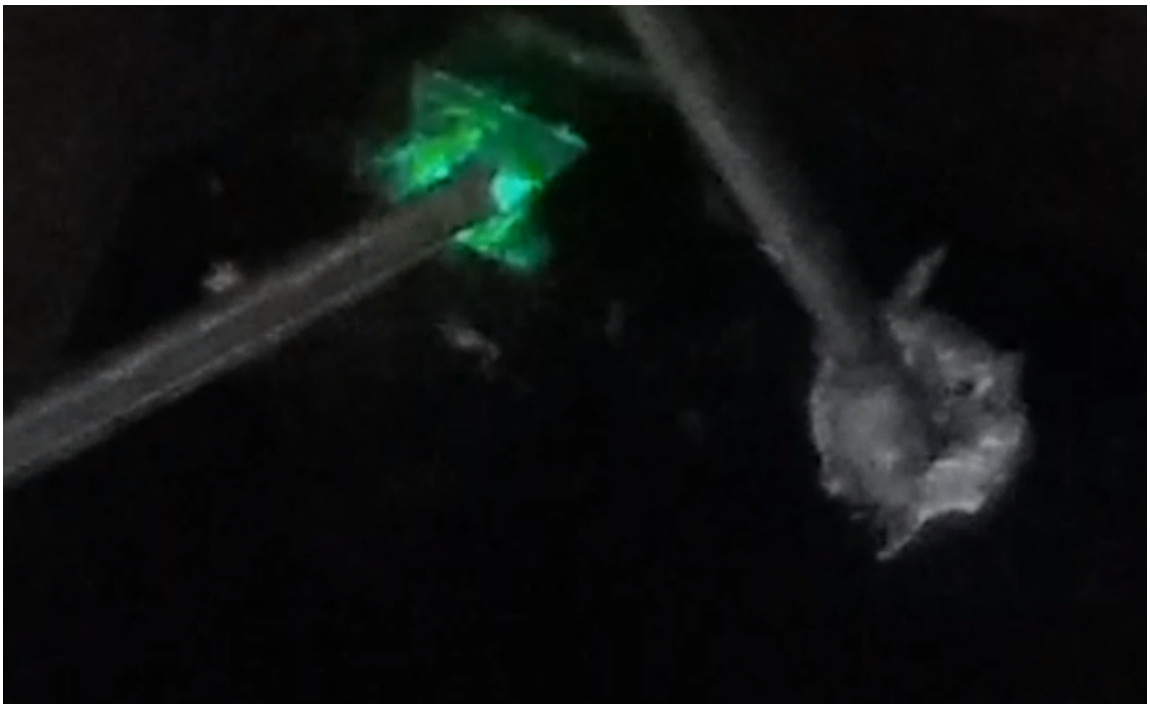

Figure 12: Electroluminescence from the 820 °C 75% specimen. The In contact for the n-GaN broke off so direct contact was made with the wire.

References

[1] Vurgaftman, I.; Meyer, J. R. *Journal of Applied Physics* **2003**, *94*, 3675–3696.

[2] Vurgaftman, I.; Meyer, J. R.; Ram-Mohan, L. R. *Journal of Applied Physics* **2001**, *89*, 5815–5875.

[3] Willardson, R. K.; Weber, E. R. In *Semiconductors and Semimetals Volume 50: Gallium Nitride (Gan) I*, 1st ed.; Moustakas, T. D., Pankove, J. I., Eds.; Academic Press: San Diego, Calif., 1998.

[4] Shibata, H.; Waseda, Y.; Ohta, H.; Kiyomi, K.; Shimoyama, K.; Fujito, K.; Nagaoka, H.; Kagamitani, Y.; Simura, R.; Fukuda, T. *MATERIALS TRANSACTIONS* **2007**, *48*, 2782–2786.

[5] Porowski, S.; Grzegory, I. *Journal of Crystal Growth* **1997**, *178*, 174–188.

[6] Moustakas, T. D.; Paiella, R. *Reports on Progress in Physics* **2017**, *80*, 106501.

[7] Auf der Maur, M.; Pecchia, A.; Penazzi, G.; Rodrigues, W.; Di Carlo, A. *Physical Review Letters* **2016**, *116*, 027401.

[8] Brandt, O.; Waltereit, P.; Ploog, K. H. *Journal of Physics D: Applied Physics* **2002**, *35*, 577.

[9] Schulz, S.; Caro, M. A.; Coughlan, C.; O'Reilly, E. P. *Physical Review B* **2015**, *91*, 035439.

[10] Jeong, H.; Jeong, H. J.; Oh, H. M.; Hong, C.-H.; Suh, E.-K.; Lerondel, G.; Jeong, M. S. *Scientific Reports* **2015**, *5*, 9373.

[11] Oliver, R. A.; Massabuau, F. C.-P.; Kappers, M. J.; Phillips, W. A.; Thrush, E. J.; Tartan, C. C.; Blenkhorn, W. E.; Badcock, T. J.; Dawson, P.; Hopkins, M. A.; Allsopp, D. W. E.; Humphreys, C. J. *Applied Physics Letters* **2013**, *103*, 141114.

[12] Armstrong, A.; Henry, T. A.; Koleske, D. D.; Crawford, M. H.; Lee, S. R. *Optics Express* **2012**, *20*, A812–A821.

A Project Story

All characterization described in this section may be found in the appendix or requested from the authors.

"Buffer" was grown on a 100 mm, (111) Si wafer. The wafer was cleaned before growth using standard SNF cleaning processes SC 1 and SC 2. The buffer recipe was adapted from a high electron-mobility GaN-on-Si transistor buffer structure with n-GaN substituted for GaN. Root-mean-squared roughness of the buffer surface was <1 nm across $\sim\mu m^2$. Presumably, the thermal and mechanical differences between n-GaN and GaN resulted in the film cracks. The wafer was kept in the inert MOCVD glovebox atmosphere so that pieces could be cleaved for growths 574-599 without additional cleaning. We cleaved and removed one piece from the glovebox for characterization, but this piece shattered during additional cleaving, so the wafer-scale crack frequency is unknown. We did not typically see cracks when imaging $\sim cm^2$ specimen surfaces grown on this buffer structure, however, so we hypothesize that the crack densities were highest near the edges due to thermal shear-stresses (Ohring, *Materials Science of Thin Films, 2nd Edition*, pp. 734). The buffer structure should be optimized for a wafer-scale processing but we do not address this here.

From pre-existing blue LED structures, and assuming that $\Delta\lambda/\Delta T$ of InGaN/GaN MQW emission is $1\,nm\,K^{-1}$ to $2\,nm\,K^{-1}$, we decided to test an initial InGaN/GaN MQW structure grown with the first 820 °C MQWs using TMIn and TEGa molar flow rates from the blue LED MQWs. The specimen was capped with nominally 50 nm n-GaN to improve photoluminescence, though the grown n-GaN thickness was significantly larger. The n-GaN cap layer was adjusted for the next growth but ultimately abandoned because its purpose was to improve PL signals but PL signals were clear, so there was no need to optimize n-GaN on InGaN/GaN MQWs. The true temperature, as measured with emissivity-corrected laser pyrometers, was adjusted for the target wavelength, and so manual adjustment of the instrument setpoint was made during the growth. The temperature schedule of the specimen is therefore considered irreproducible. PL was blue-green, and so the temperature was lowered for the next growth to increase In incorporation.

The 800 °C MQW low-temperature growth resulted in what is suspected to be highly-defective yellow emission in PL. After deciding not to pursue the n-GaN cap, the 820 °C MQW without the manual temperature adjustments was regrown to improve the measurement from the first 820 °C MQW. The 820 °C MQW had a peak wavelength near the target 530 nm wavelength, and so we decided to initially use this MQW recipe with p-GaN caps to create a simple green MQW LED structure.

820 °C Purple LED, 820 °C Green LED, and 800 °C Yellow LED are the results of capping previous MQW structures with p-GaN. For 820 °C Purple LED, the 820 °C MQW structure apparently degraded during high-temperature (∼980 °C true temperature) p-GaN capping. This caused the photoluminescence to blue-shift significantly. We also targeted 250 nm of p-GaN, but literature searches showed this was not necessary, and so we lowered both p-GaN temperature and growth time. We used the ∼820 °C MQW recipe again with a true p-GaN temperature of ∼930 °C and with less p-GaN growth time to produce 820 °C Green LED. This p-GaN cap was ∼120 nm thick and the PL was only slightly blue-shifted from 820 °C MQW. Assuming that the 800 °C MQW spectra might also blue-shift, we grew the 800 °C MQW recipe with ∼930 °C p-GaN, adjusting growth time even lower for ∼100 nm. This growth, however, remained defective and yellow.

We decided to try the low-temperature p-GaN growth with the 820 °C MQW growth parameters, except we lowered the growth temperature to 810 °C. Additionally, however, we grew three specimens with different TMIn/(TEGa+TMIn) molar flow ratios: 810 °C 75%, 810 °C 90%, and

810 °C 70%. 810 °C 75% used the same III ratio as all the previous growths. TMIn flow was varied to determine if TMIn incorporation was saturated at 810 °C and how it affected PL wavelengths. The 810 °C 90% specimen appeared to be defective in PL and SEM. We hypothesize that this was due to significant In and/or InN during the InGaN growth. We grew an 810 °C 75% to complete the two-factor experiment. There are hold times at MQW interfaces where the temperature is allowed to stabilize at the quantum well or quantum barrier temperature, and these were left in even for the constant-temperature experiments. However, we performed an experiment that reduced these hold times in order to test if PL intensity was improved, presumably due to reduce contamination deposition at the interface, which it was. Finally, we also performed an experiment with these hold times but with a 50 °C higher temperature in the GaN quantum barriers, which also increase photoluminescence intensity.

B Material Characterization

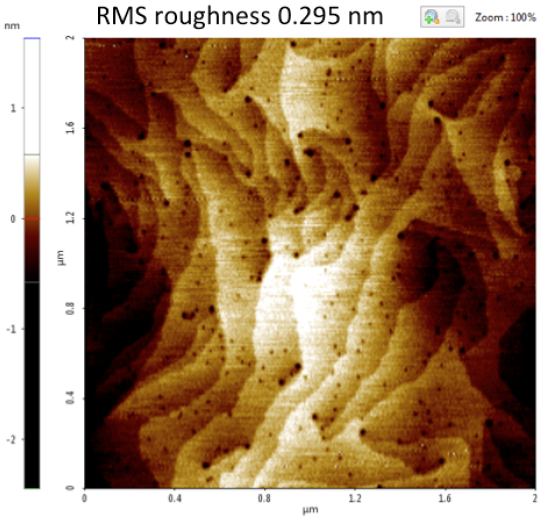

(a) 572

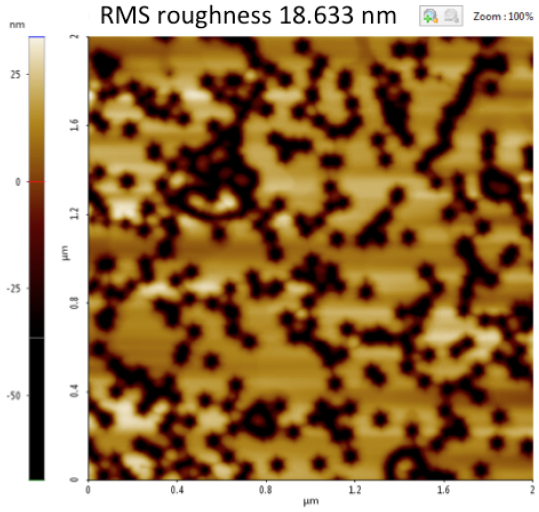

(b) 574

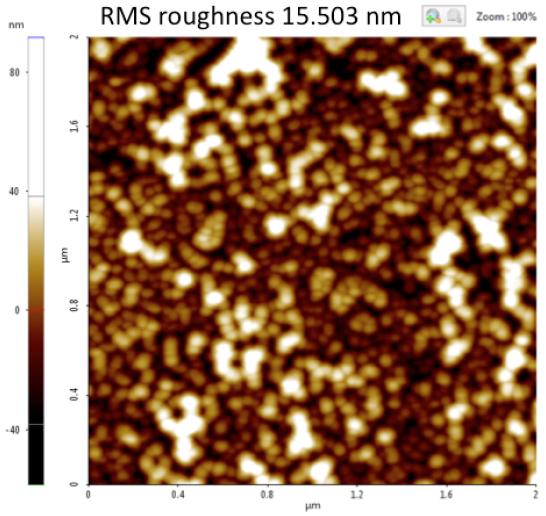

(c) 578

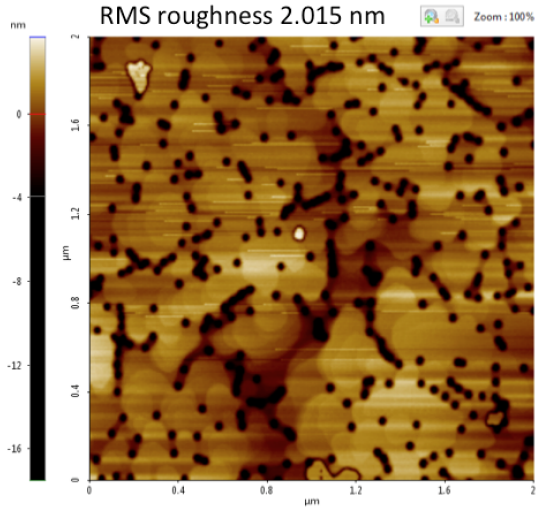

(d) 580

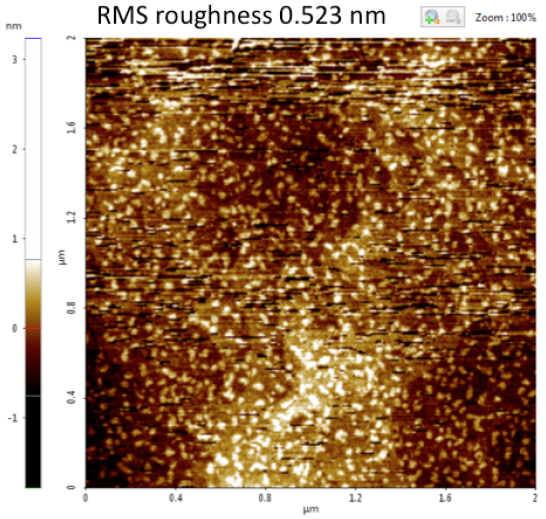

(e) 582

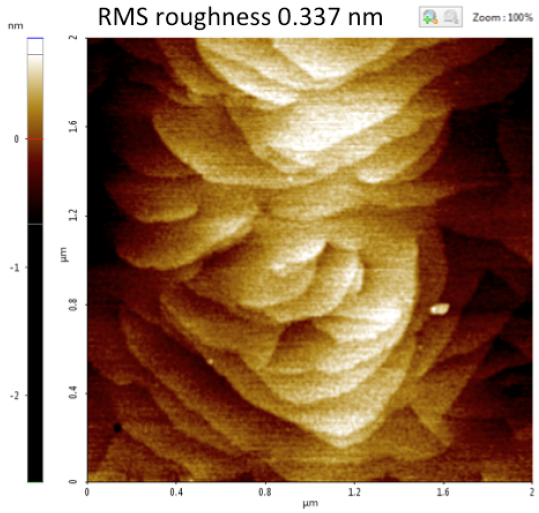

(f) 586

Figure 13: AFM profiles.

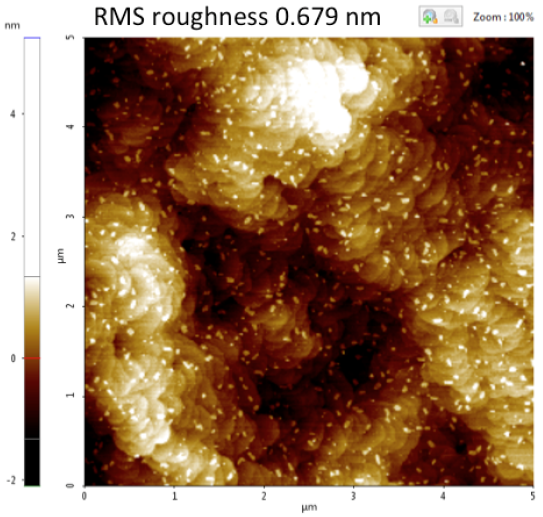

(a) 586

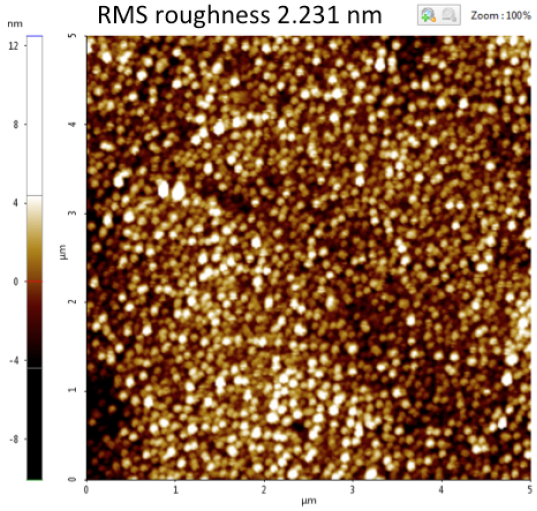

(b) 590

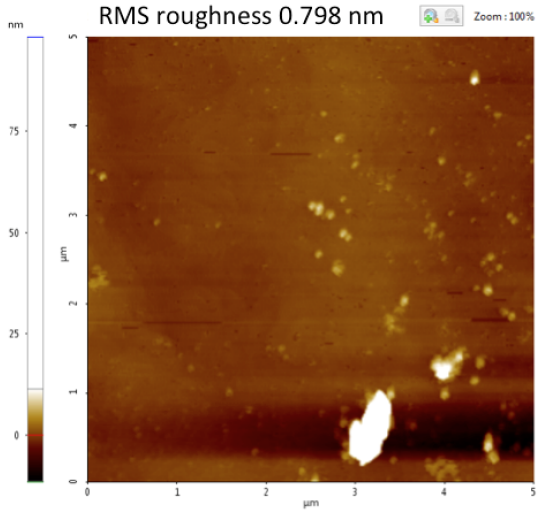

(c) 595

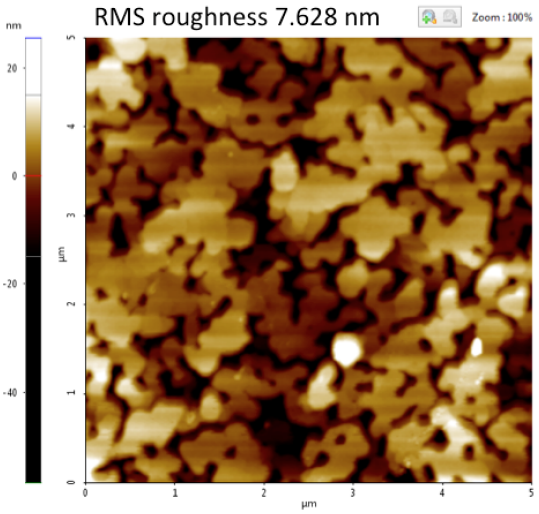

(d) 597

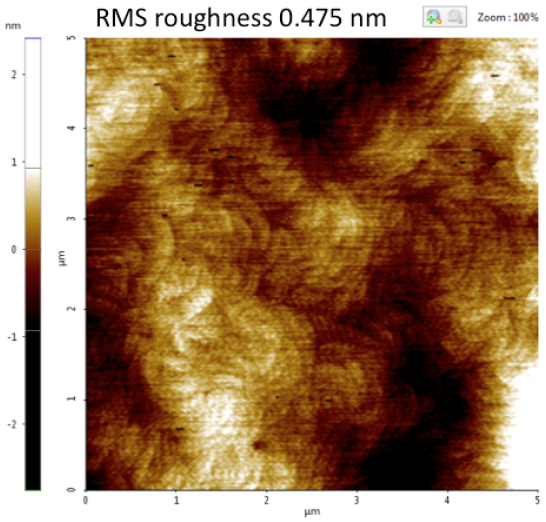

(e) 599

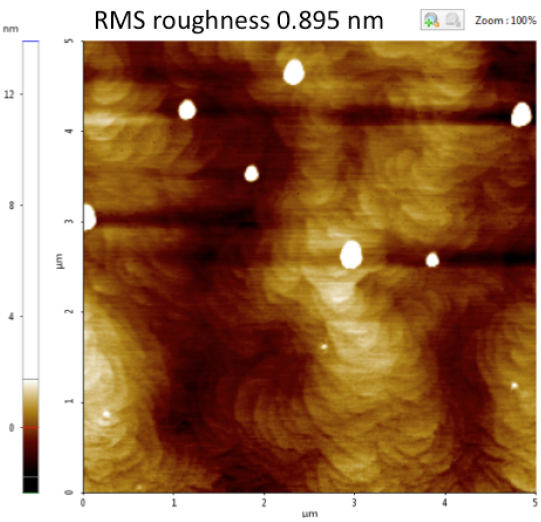

(f) 612

Figure 14: AFM profiles.

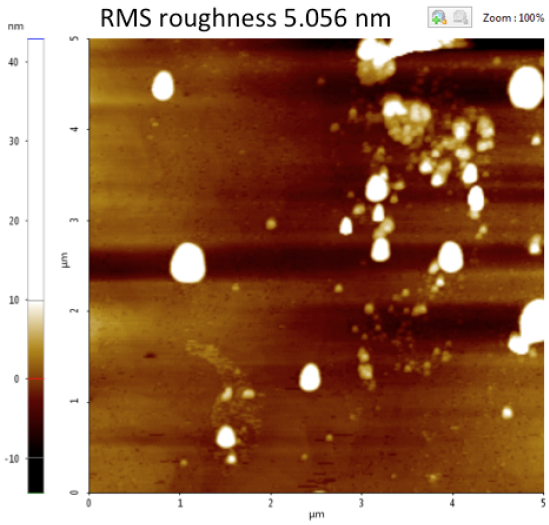

(a) 616

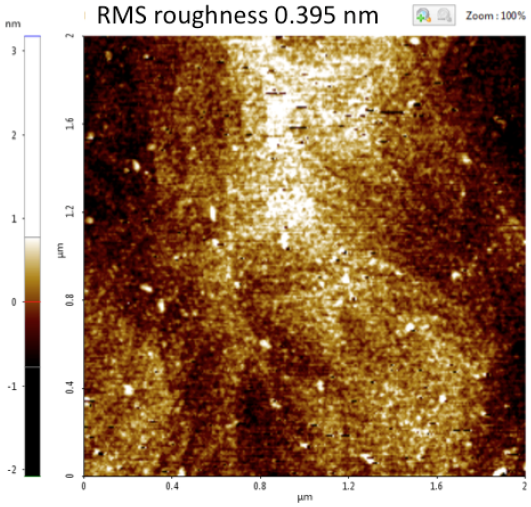

(b) Blue LED from which our recipes began.

Figure 15: AFM results.

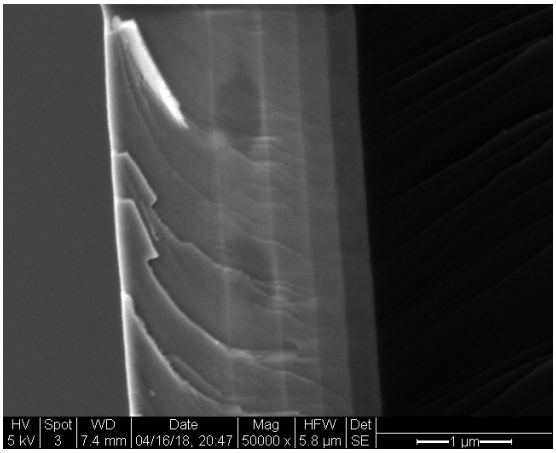

(a) 572

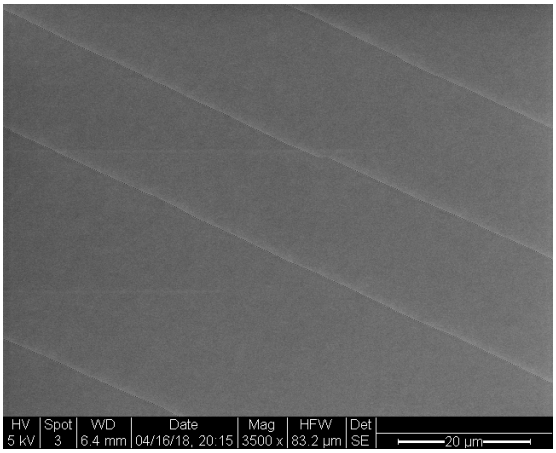

(b) 572

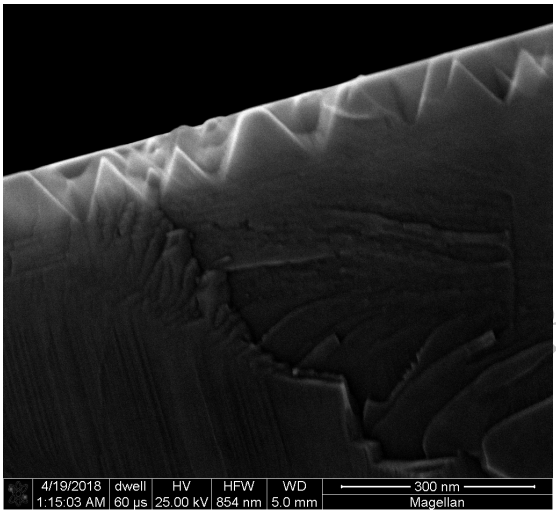

(c) 574

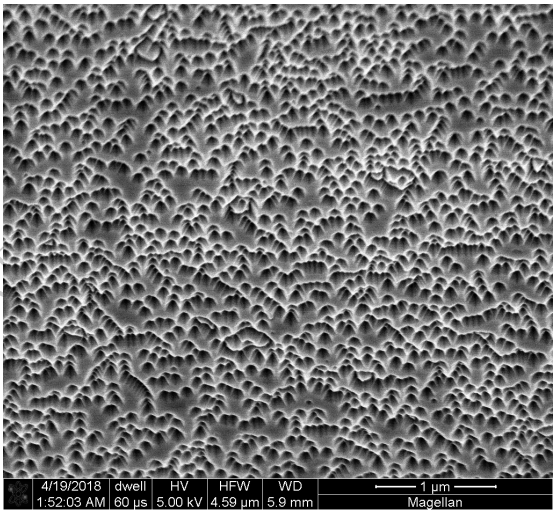

(d) 574

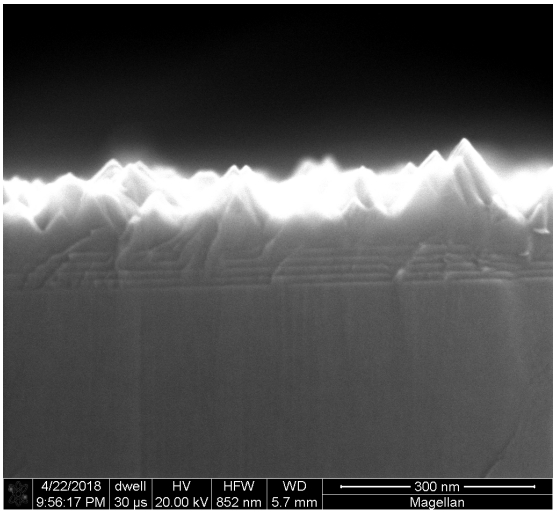

(e) 578

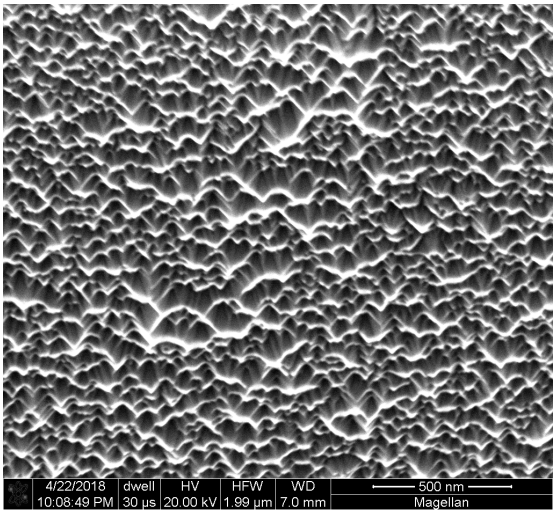

(f) 578

Figure 16: SEM micrographs.

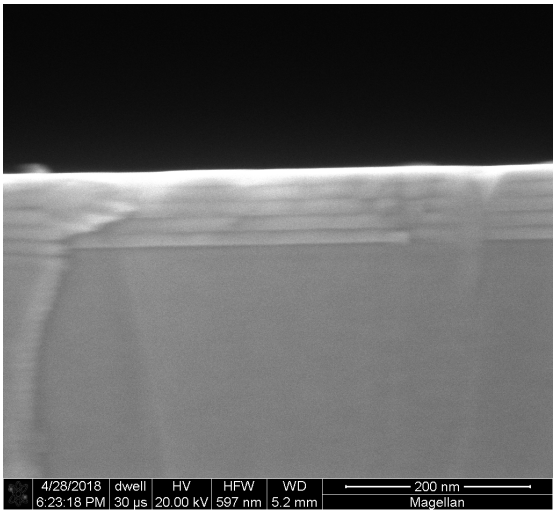

(a) 580

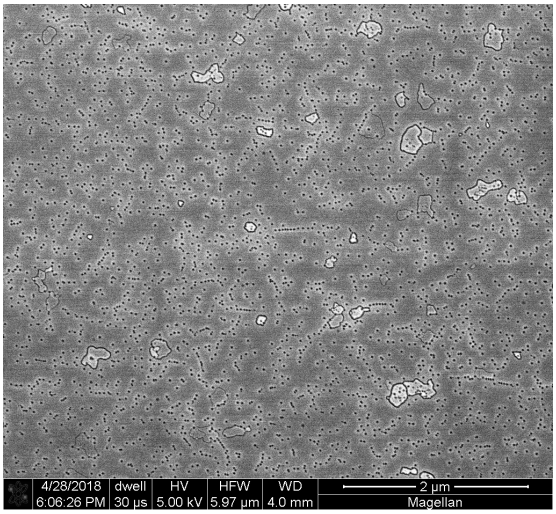

(b) 580

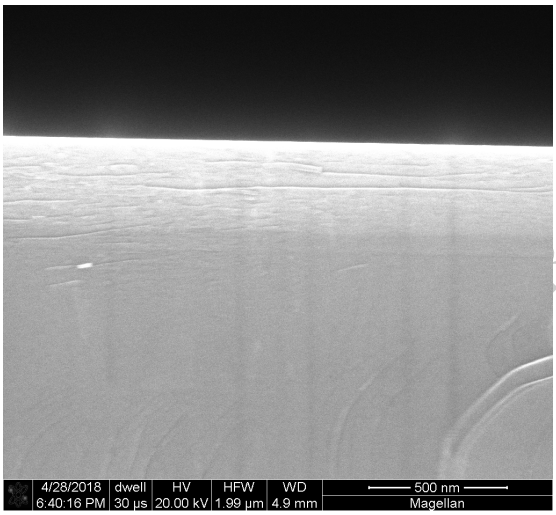

(c) 582

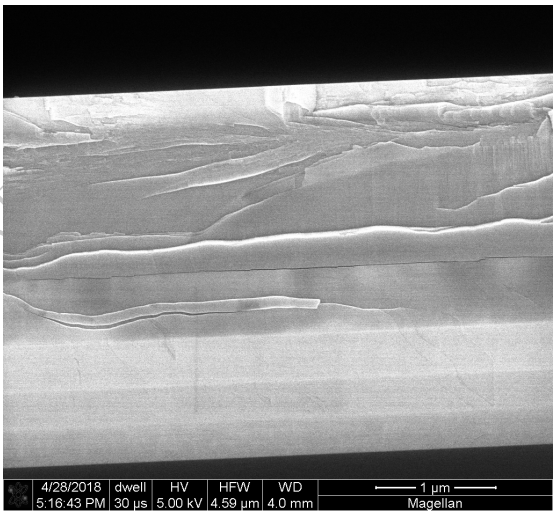

(d) 582

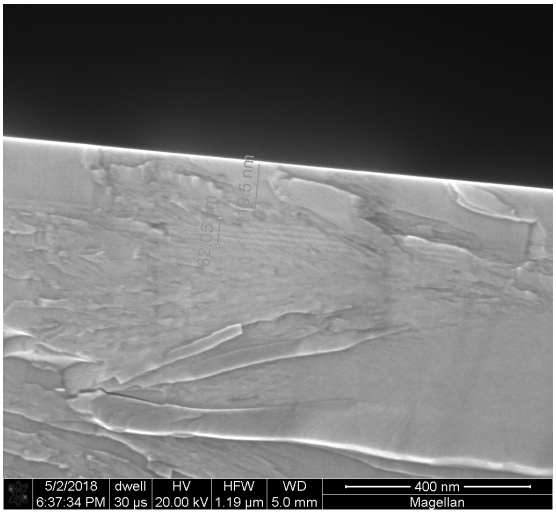

(e) 586

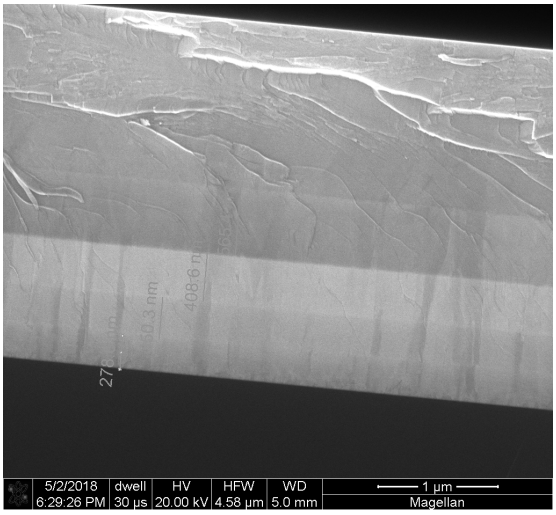

(f) 586

Figure 17: SEM micrographs.

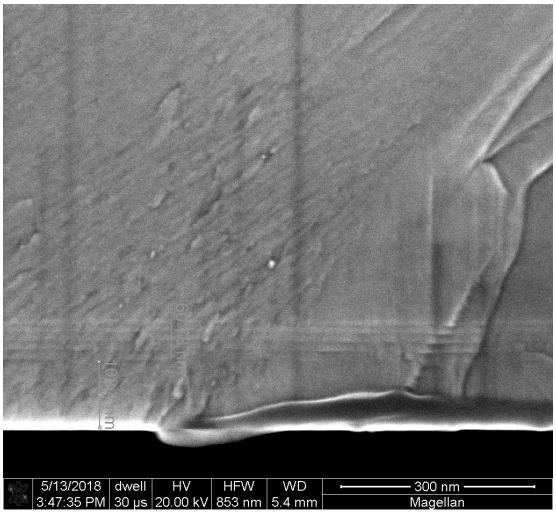

(a) 590

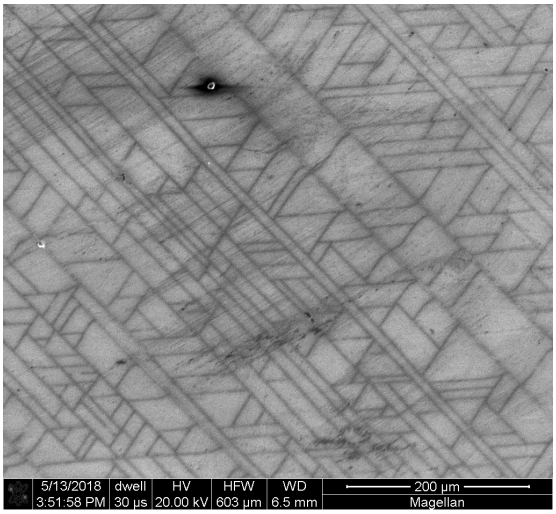

(b) 590

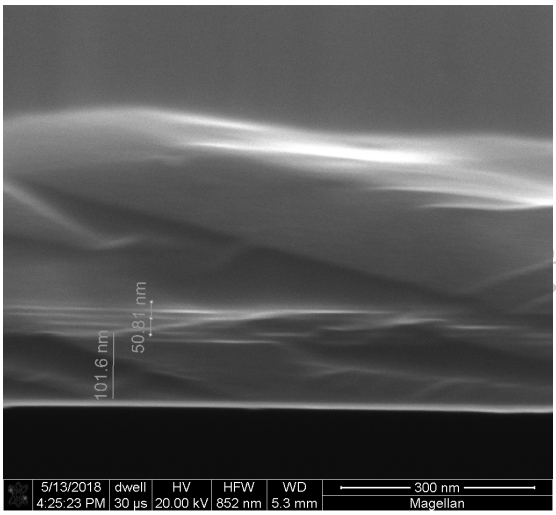

(c) 595

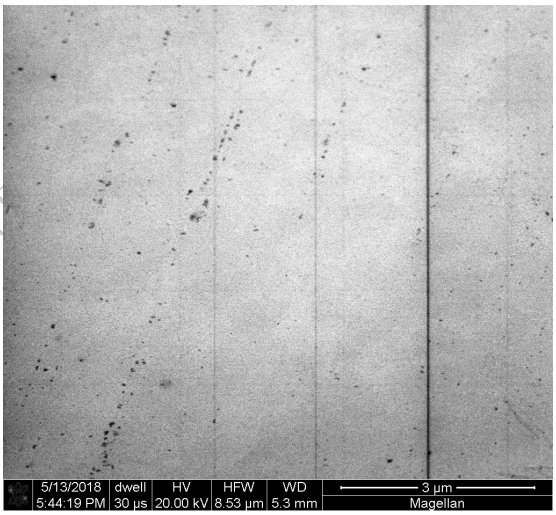

(d) 595

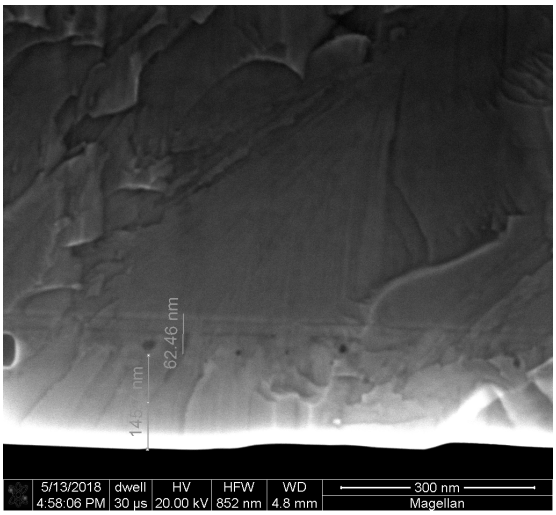

(e) 597

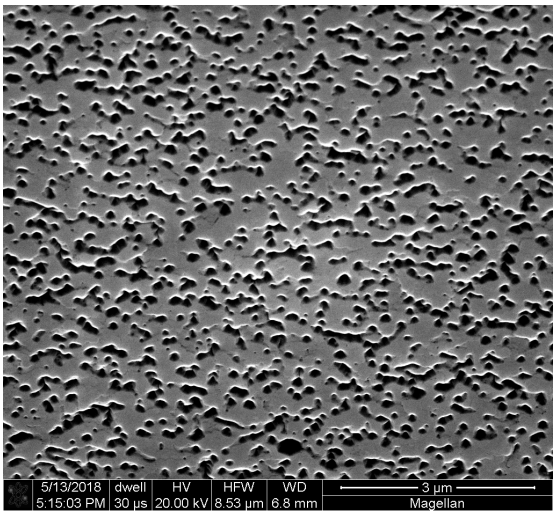

(f) 597

Figure 18: SEM micrographs.

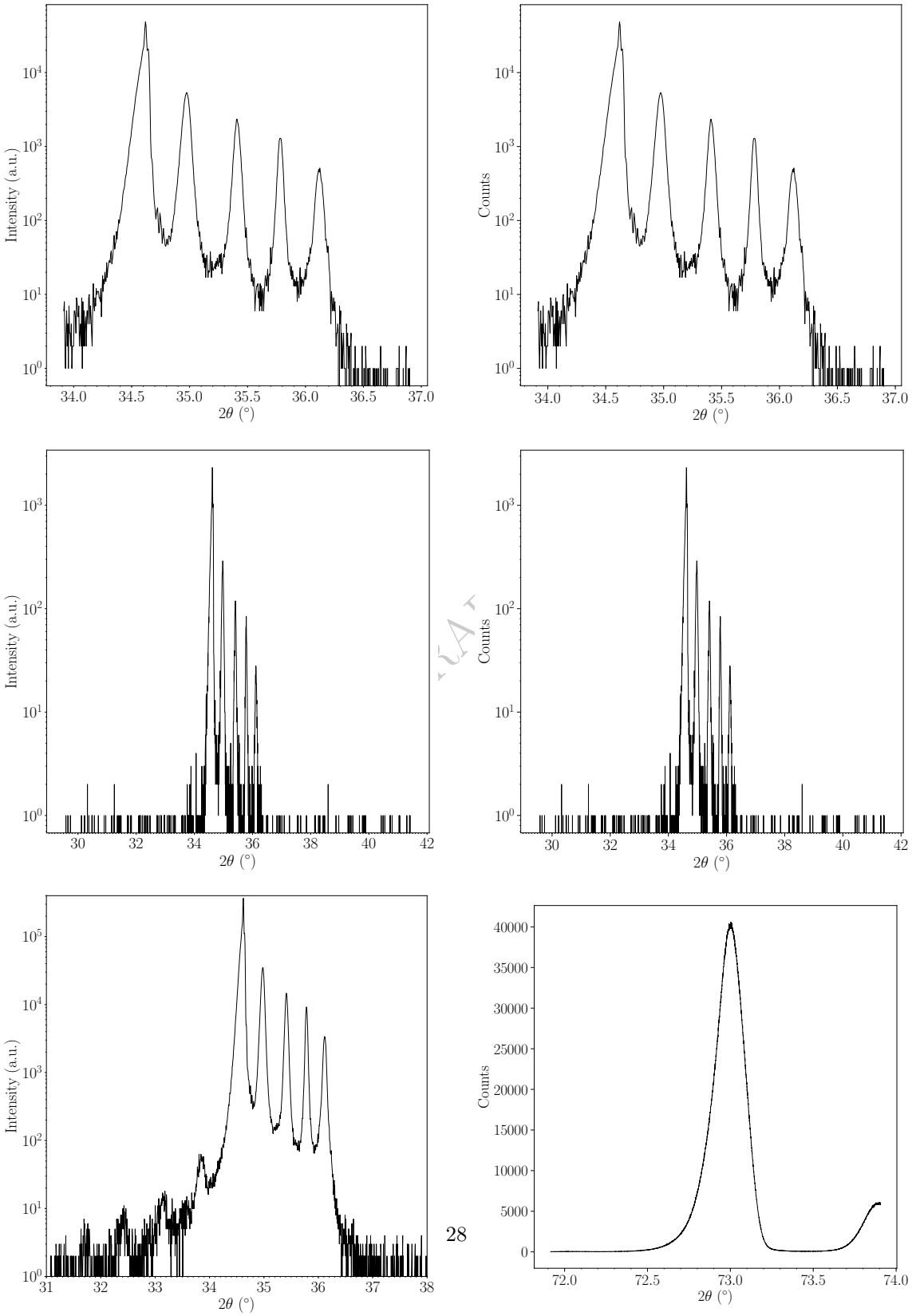

Figure 19: Original blue LED XRD. This recipe was modified for our work.

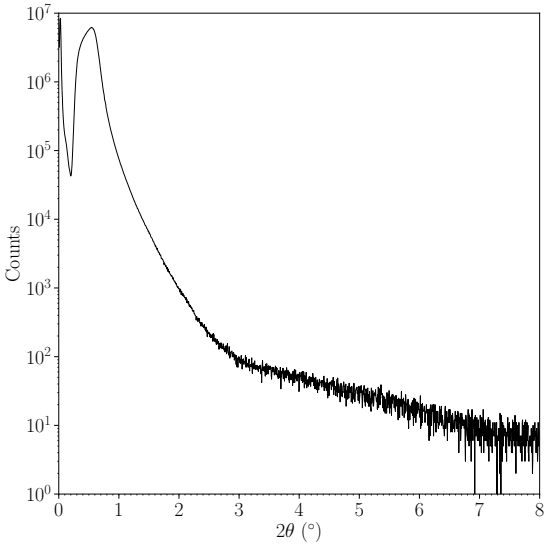

Figure 20: Original blue LED x-ray reflectivity. This recipe was modified for our work.

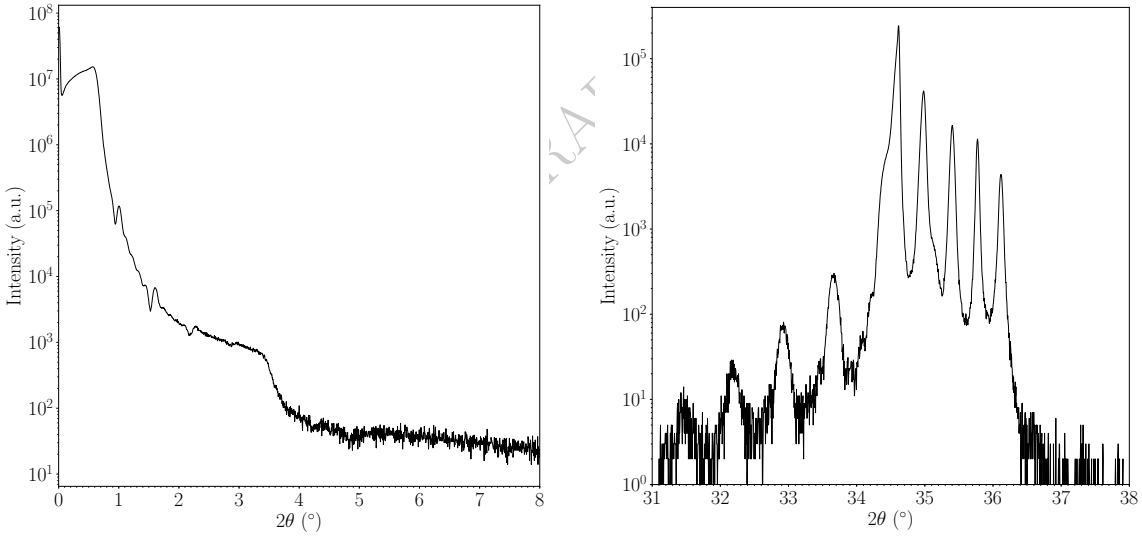

Figure 21: 580 XRD and x-ray reflectivity

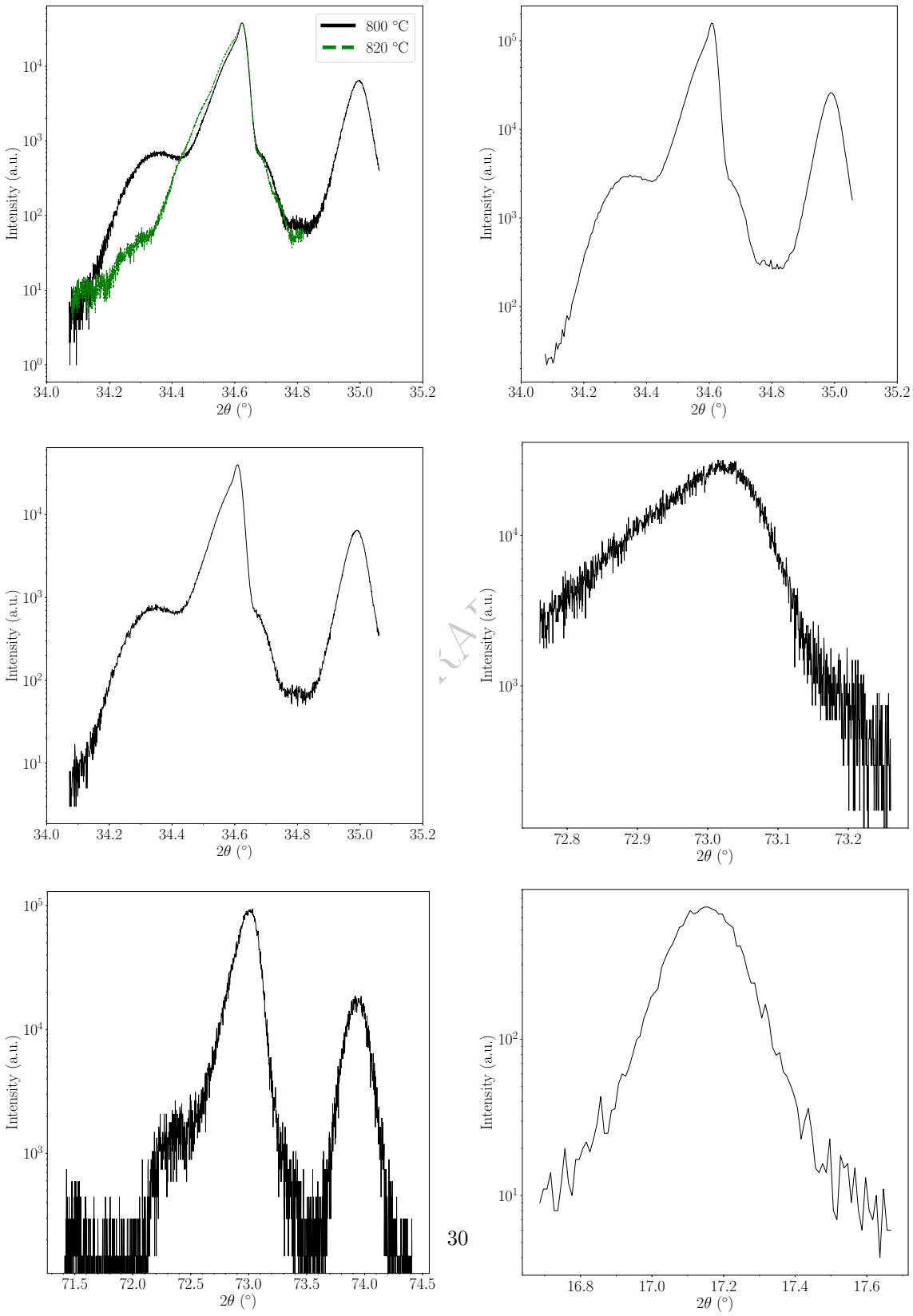

Figure 22: 578 XRD

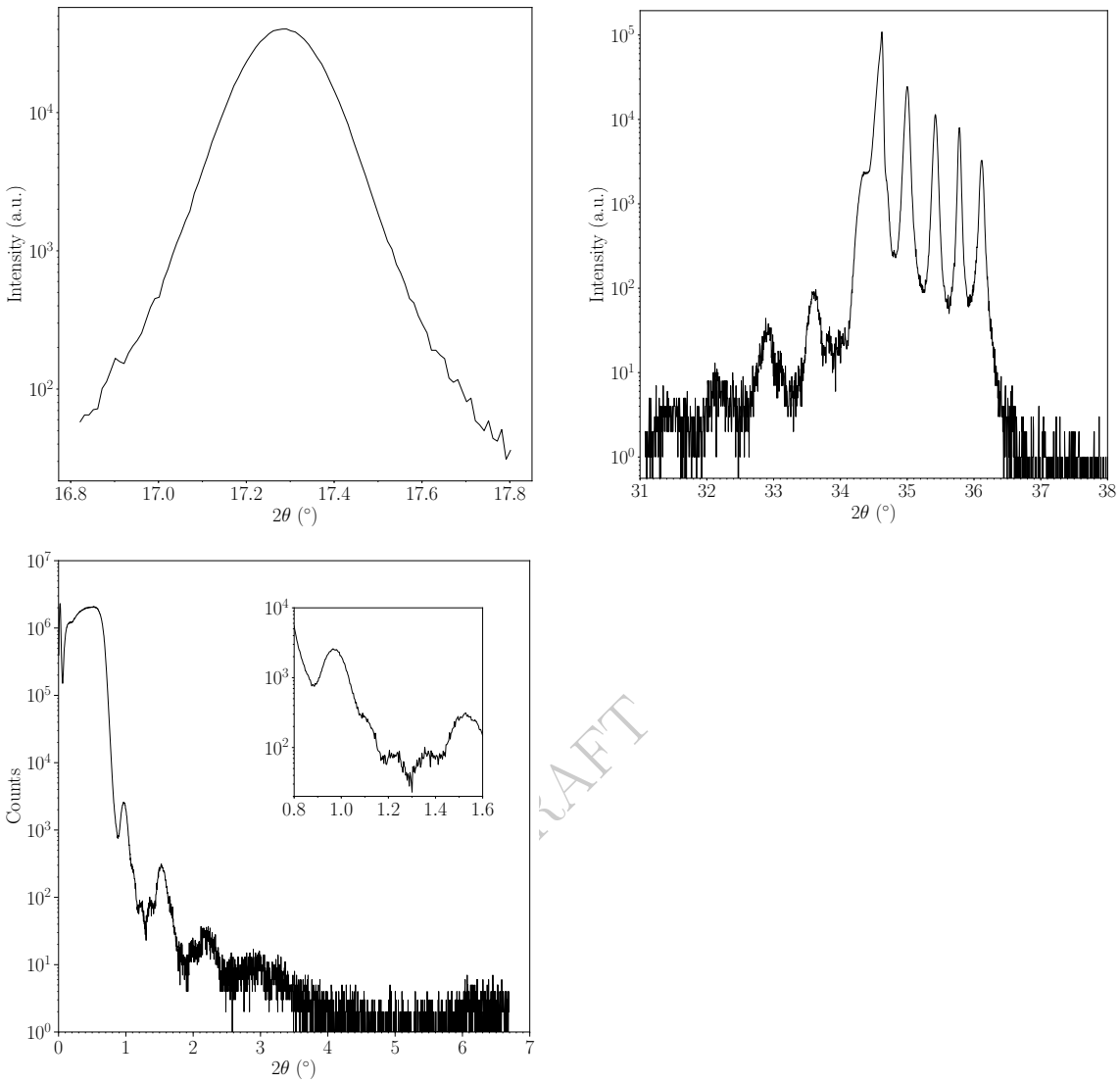

Figure 23: 578 XRD and x-ray reflectivity

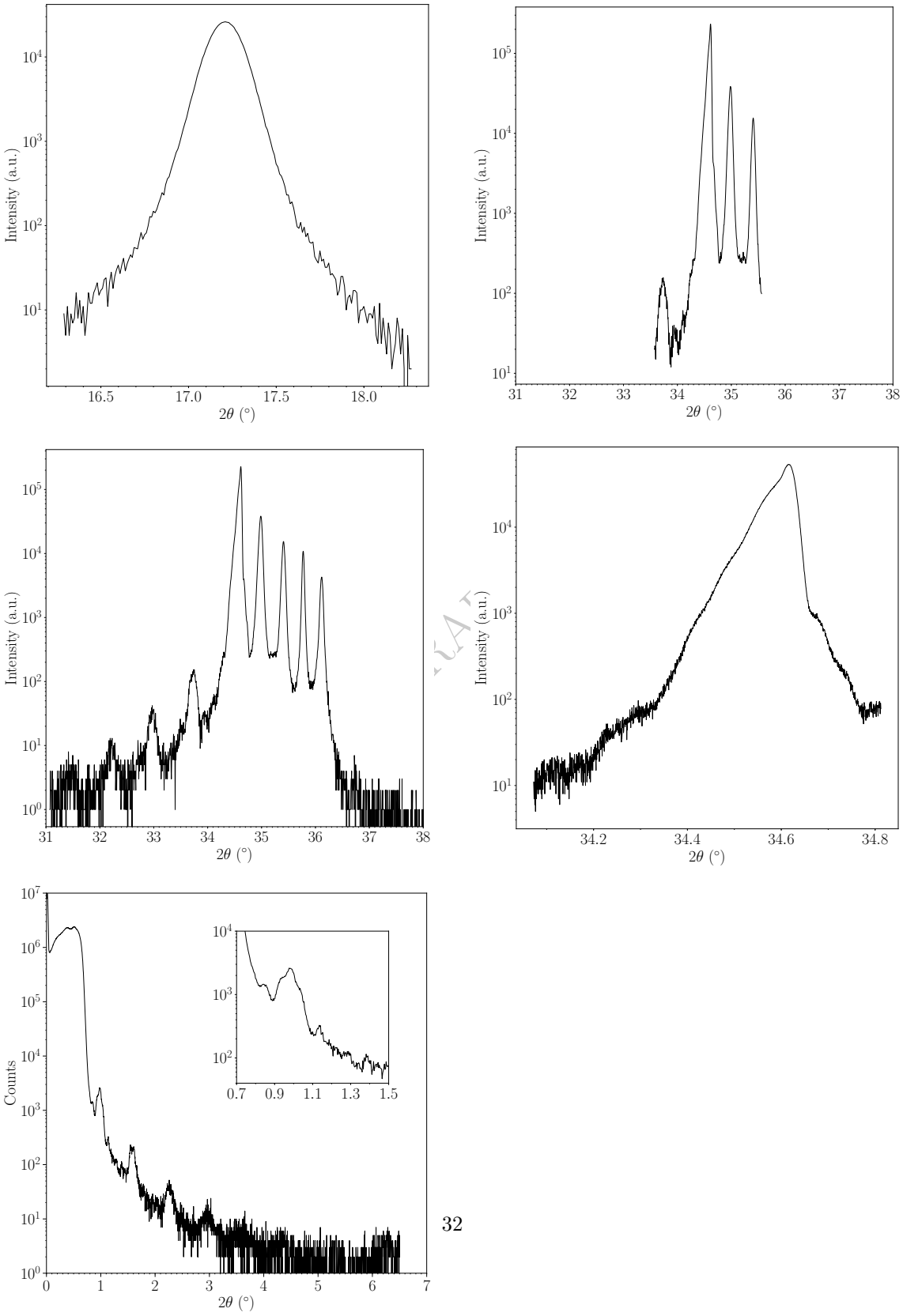

Figure 24: 574 XRD and x-ray reflectivity

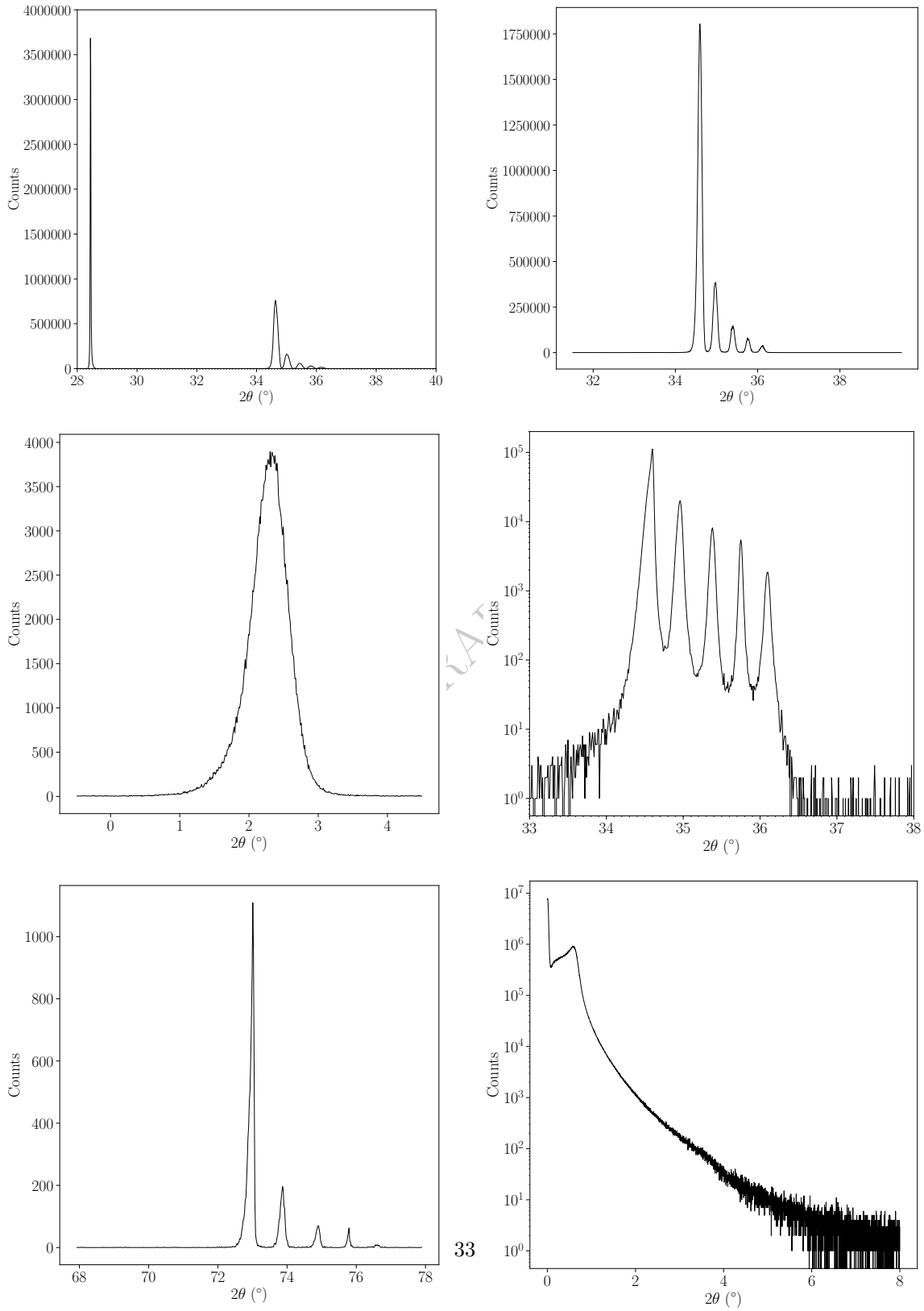

Figure 25: 572 XRD and x-ray reflectivity

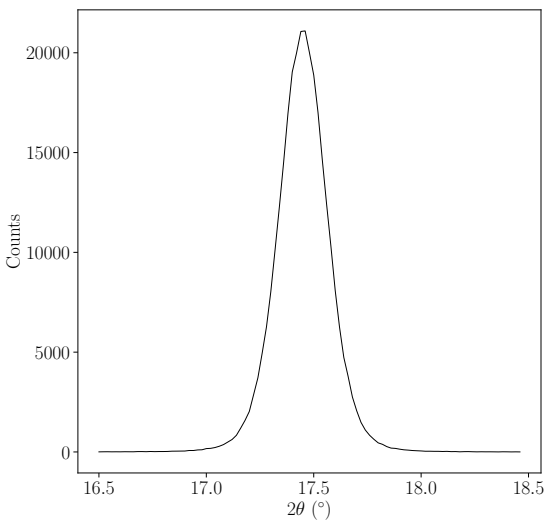

(a) $Al_{0.2}Ga_{0.8}N$

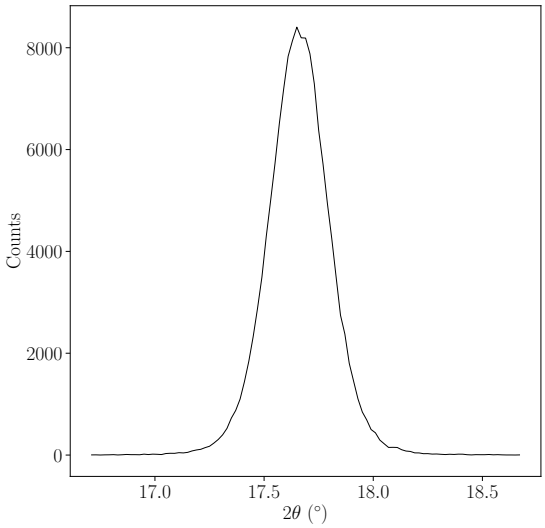

(b) $Al_{0.5}Ga_{0.5}N$

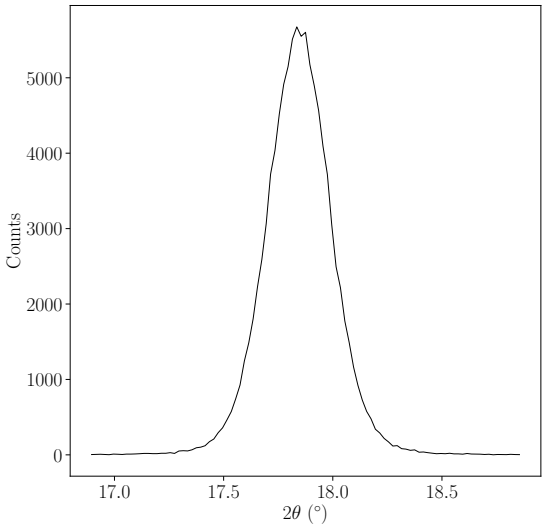

(c) $Al_{0.8}Ga_{0.2}N$

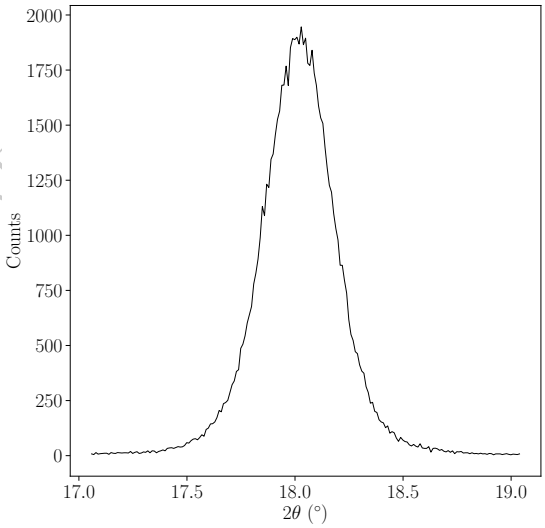

(d) AlN

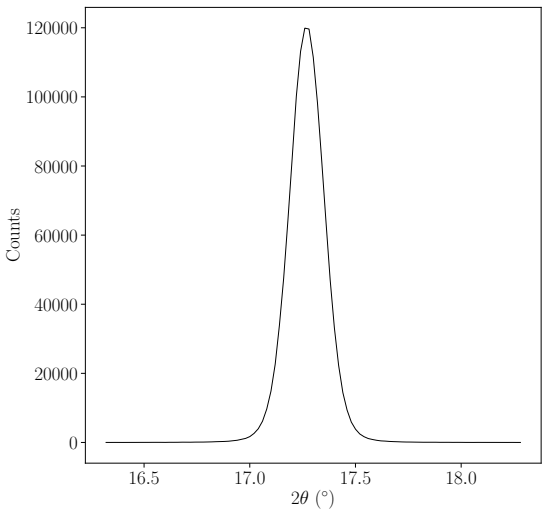

(e) n-GaN

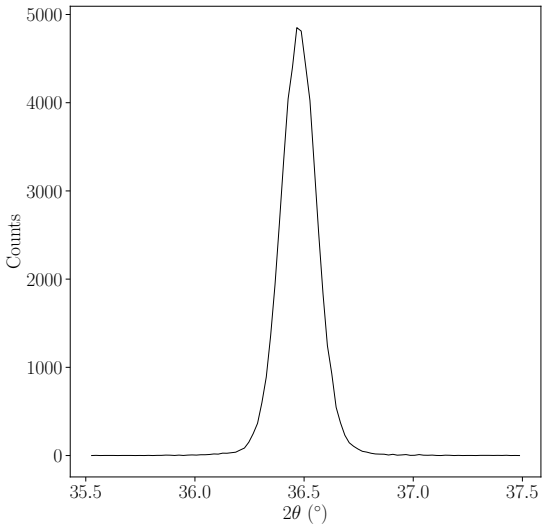

(f) n-GaN, (004) peak

Figure 26: Rocking curves for buffer structure (002) peaks, unless noted. The diffractometer was moved to the peaks maximums shown in symmetric-radial scans and rocked in ω with a triple-axis

C Code

All figures were created with Python 2.7, using data files provided by the instrument computers.

C.1 Photoluminescence

Signal vs. λ can be exported in .csv format by selecting the two data columns in the final experimental result screen and exporting via the "File" menu.

```
import matplotlib.pyplot as plt
import numpy as np
import csv
from matplotlib import rc

### DATA 1 ###

from matplotlib.ticker import MultipleLocator

# for TeX

rc('font', **{'family': 'serif', 'serif': ['Computer Modern']})
rc('text', usetex=True)

intensity, wavelength, energy = [], [], []

# read in wavelength and intensity from .csv file.

with open('/file/path/'\
          '595_60degrees.csv', 'rb') as csvfile:
    spamreader = csv.reader(csvfile, delimiter=',')
    for row in spamreader:
        wavelength.append(float(row[0]))
        intensity.append(float(row[1]))

energy = np.divide(1240.0,wavelength)

### PLOTTING ###

fig = plt.figure(figsize=(10,10))
axes = fig.add_axes([0, 0, 1, 1]) # left, bottom, width, height (range 0 to 1)

# plot aesthetics
axes.set_xlabel(r"Wavelength~(nm)",size=30)
axes.set_ylabel("Intensity (a.u.)",size=30)
#axes.set_yscale("log")
#axes.set_xlim(400,750)
#axes.set_xlim(0.6,1.1)
```

```
axes.tick_params(axis='both', labelsize=30, pad=0)
axes.get_yaxis().set_tick_params(which='major',
             direction='out',width=1, size=7)
axes.get_xaxis().set_tick_params(which='major',
             direction='out',width=1, size=7)
#axes.xaxis.set_minor_locator(ml)

# create minor ticks on x-axis
#axes.xaxis.set_minor_locator(ml)

# create minor ticks on x-axis
ml = MultipleLocator(10)
axes.xaxis.set_minor_locator(ml)
#ml = MultipleLocator(1000)
#axes.yaxis.set_minor_locator(ml)

wavelength = np.array(wavelength)
intensity = np.array(intensity)

p1, = axes.plot(wavelength, [i-min(intensity) for i in intensity], '-.',
      color='blue', markersize=1, label = r'810 $^\circ$C, 75$\%$')

### DATA 2 ###

intensity, wavelength, energy = [], [], []

with open('/file/path/'\
          '626_60degrees.csv', 'rb') as csvfile:
    spamreader = csv.reader(csvfile, delimiter=',')
    for row in spamreader:
        wavelength.append(float(row[0]))
        intensity.append(float(row[1]))

energy = np.divide(1240.0,wavelength)

p2, = axes.plot(wavelength, [(i-min(intensity))for i in intensity], '-',
      color='black', markersize=1, label = r'Smaller Holds')

intensity, wavelength, energy = [], [], []

with open('/file/path/'\
          '630_60degrees.csv', 'rb') as csvfile:
    spamreader = csv.reader(csvfile, delimiter=',')
    for row in spamreader:
        wavelength.append(float(row[0]))
        intensity.append(float(row[1]))
```

```
energy = np.divide(1240.0,wavelength)

p3, = axes.plot(wavelength, [(i-min(intensity))for i in intensity], '--',
      color='green', markersize=1, label = 'Barrier $\Delta$ T= 50$^\circ$C')

### TEXT ###

#right = 0.9
#top = 0.9

#axes.text(0.42, 0.7, "Some Text", horizontalalignment='right',
#   verticalalignment='top', transform=axes.transAxes, fontsize=30)
#axes.text(0.75, 0.5, "Some Text", horizontalalignment='right',
#   verticalalignment='top', transform=axes.transAxes, fontsize=30)

### LEGEND ###

leg =( axes.legend([p1, p2, p3], [r'810 $^\circ$C, 75\%',
           r'Shorter Holds', 'QB $\Delta$ T= 50$^\circ$C'], loc=1,
           prop={'size':30}))

for legobjs in leg.legendHandles:
    legobjs.set_linewidth(7.0)

### SHOW, SAVE, CLOSE ###
plt.show()
fig.savefig("/file/path/'\
            'extras.pdf", bbox_inches='tight', dpi=600)
plt.close()
```


C.2 Reciprocal Space Mapping

Used to plot .csv files generated by the X'Pert diffractometers. RSM .xrdml files may be converted to .csv using the X'Pert's "Data Viewer" software via the "File" menu.

```
  from matplotlib import colors
import matplotlib.pyplot as plt
import numpy as np
import csv
from mpl_toolkits.axes_grid1 import make_axes_locatable
from matplotlib import rc
from matplotlib.mlab import griddata
import matplotlib.ticker as plticker

rc('font', **{'family': 'serif', 'serif': ['Computer Modern']})
rc('text', usetex=True)
```

```
def rsm_plotter(directory_name, file_name):
    all_points, converted_points = [], []

    wavelength = 1.54 # Angstroms

    # read in two theta and intensity from .csv file.
    with open('%s%s.csv' % (directory_name, file_name), 'rb') as csvfile:
        spamreader = csv.reader(csvfile, delimiter=',')
        for row in spamreader:
            if row[0] == '2Theta position':
                break
        for row in spamreader:
            #2theta, omega, intensity
            all_points.append([float(row[0])*np.pi/180,
                               float(row[1])*np.pi/180, float(row[2])])

    # convert from omega two theta space to d-spacing

    converted_points = [[np.abs(wavelength/(-np.cos(i[1]-i[0])+np.cos(i[1]))),
                         np.abs(wavelength/(-np.sin(i[1]-i[0])+np.sin(i[1]))),
                         i[2]] for i in all_points]

    d_par = [np.round(i[0], decimals=3) for i in converted_points]
    d_perp = [i[1] for i in converted_points]
    intensity = [i[2] for i in converted_points]
    new_intensity = [i+0.1 for i in intensity]

    #Plotting

    fig = plt.figure(figsize=(10,10))
    axes = fig.add_axes([0, 0, 1, 1])

    # define grid.
    xi = np.linspace(min(d_par), max(d_par), 2000)
    yi = np.linspace(min(d_perp), max(d_perp), 2000)

    # grid the data.
    #zi = griddata((d_par, d_perp), new_intensity, (xi[None,:],
    #     yi[:,None]), method = "cubic")

    zi = griddata(d_par, d_perp, new_intensity, xi, yi, interp = "linear")
    # contour the gridded data,
    # plotting dots at the randomly spaced data points.

    ax = axes.imshow(zi, extent = [min(d_par), max(d_par), min(d_perp),
```

```
     max(d_perp)], origin = 'lower', aspect='auto',
     norm = colors.LogNorm(), cmap = "bwr")

axes.contour(zi, extent = [min(d_par), max(d_par), min(d_perp),
     max(d_perp)], origin = 'lower', aspect='auto',
     levels=np.logspace(2, 5, 10), colors = 'black')

# Draw lines for constant or linear d-spacings
axes.plot([2.762, 2.762], [1.03,1.07], color='black',
          linestyle='--', linewidth=2)

axes.plot([2.762, 2.762+(3.059-2.762)*.2],
           [1.0371,1.0371+(1.1386-1.0371)*.2], color='black',
           linestyle='--', linewidth=2)

axes.set_xlabel(r'd$_\parallel$ (\r{A})', size = 30)
axes.set_ylabel(r'd$_\bot$ (\r{A})', size = 30)
plt.text(2.784, 1.058, r'In$_x$Ga$_{1-x}$N$', size = 30)
plt.text(2.72, 1.071, r'(100) GaN', size = 30)

# ticks may need to be adjusted
#axes.set_xticks(arange(32.7,33.3,0.1))
axes.tick_params(axis='both', labelsize=30, pad=5)
#axes.set_xlim(4.1,4.25)
#axes.set_ylim(1.16,1.18)
#axes.set_facecolor('black')
#axes.contour([0,1000])
axes.get_yaxis().set_tick_params(which='both', direction='out', size = 7)
axes.get_xaxis().set_tick_params(which='both', direction='out', size = 7)
#loc = plticker.MultipleLocator(base=0.005)

loc = plticker.MultipleLocator(base=0.02)
axes.xaxis.set_minor_locator(loc)
loc = plticker.MultipleLocator(base=0.002)
axes.yaxis.set_minor_locator(loc)
 # this locator puts ticks at regular intervals
#axes.yaxis.set_minor_locator(loc)

# create minor ticks on x-axis
#axes.xaxis.set_minor_locator(ml)
divider = make_axes_locatable(axes)
cax = divider.append_axes("right", size="5%", pad=0.3)
cax.set_ylabel('',size = 30, labelpad = 10)
cax.tick_params(axis='both', pad = 5, labelsize=30)

plt.colorbar(ax, cax=cax, label = r'Intensity (a.u.)')
```

```
    # show, save, and close plots
    plt.savefig("%s%s.pdf" % (directory_name, file_name),
                bbox_inches='tight', dpi=400)
    plt.show()
    plt.close()

beam_energy = rsm_plotter("/file/path/","file_name")
```